

AUS Repository

LoRa Sub Milliwatt Transceiver Design to Reduce Space Solutions Mass

Item Type	Thesis
Authors	Ali, Hessa
Download date	2026-06-13 09:58:18
Link to Item	http://hdl.handle.net/11073/24283

LORA SUB MILLIWATT TRANSCEIVER DESIGN TO REDUCE SPACE
SOLUTIONS MASS

by

Hessa Ali Hussain Ahmed Ali

A Thesis Presented to the Faculty of the
American University of Sharjah
College of Engineering
In Partial Fulfillment
of the Requirements
for the Degree of

Master of Science in
Electrical Engineering

Sharjah, United Arab Emirates

MAY 2022

Declaration of Authorship

I declare that this Thesis is my own work and, to the best of my knowledge and belief, it does not contain material published or written by a third party, except where permission has been obtained and/or appropriately cited through full and accurate referencing.

Signed.....Hessa Ali Hussain.....

Date.....26/May/2022.....

The Author controls copyright for this report.

Material should not be reused without the consent of the author. Due acknowledgement should be made where appropriate.

© Year 2022

Hessa Ali Hussain Ahmed Ali

ALL RIGHTS RESERVED

Approval Signatures

We, the undersigned, approve the Master's Thesis of Hessa Ali Hussain Ahmed Ali

Project Title: LORA SUB MILLIWATT TRANSCEIVER DESIGN TO REDUCE SPACE SOLUTIONS MASS

Date of Defense: 17/MAY/2022

Name, Title and Affiliation

Signature

Dr. Lutfi Albasha
Associate Professor, Department of Electrical Engineering
Thesis Advisor

Dr. Nasser Qaddoumi
Associate Professor, Department of Electrical Engineering
Thesis Committee Member

Dr. Abdul-Rahman Al-Ali
Associate Professor, Department of Computer Science and
Engineering
Thesis Committee Member

Dr. Oualid Hammi
Head or Program Director
Department of Electrical Engineering

Dr. Lotfi Romdhane
Associate Dean for Graduate Affairs and Research
College of Engineering

Dr. Fadi Aloul
Dean
College of Engineering

Dr. Mohamed El-Tarhuni
Vice Provost for Graduate Studies
Office of Research and Graduate Studies

Acknowledgement

I would like to thank my advisor Dr. Lutfi Albasha for providing knowledge, guidance, support, and motivation throughout my research stages. I'm deeply beholden for his great assistance, worthy discussion, and suggestions.

I would like to thank my organization Mohammed Bin Rashed Space Centre (MBRSC) for their continuous support. I really appreciate their dignified motivation during my graduate study.

Abstract

Space sector is a popular research area. The world is trying to launch different space solutions to improve our life. However, the price of launching any solution is extremely expensive as the price is directly proportional to the mass of the spacecraft and its subsystems. In order to have space accessible to more developers, the design of the spacecraft needs to be optimized to reduce the mass as much as possible. One of the main contributors to this high mass is the harness of the satellite which carries the data within the spacecraft. Thus, the main objective of this research is to introduce an ultra-low power consumption (sub-milli-watt) transceiver using LoRa (Long Range) technology. Specifically, focusing on designing small size transceiver to be used inside CubeSats with minimum possible power consumption that works in Industrial, Scientific and Medical (ISM) band to replace the harness. The design of this Mini Printed Circuits Board (PCB) transceiver is modular to fit any existing PCB designs in the market to be able to collect all the data using Inter-Integrated Circuit (I2C) and distribute it by small antenna using LoRa scheme. The data can be formatted in anyway then received by the mini transceiver to be processed and distributed around the different CubeSat subsystems using LoRa. The solution proposed in this research is unique as it has never been addressed in space applications before, to the best knowledge of the author.

Keywords: Long range; printed circuits board; ISM; I2C.

Table of Contents

Abstract	5
List of Figures	9
List of Tables	11
List of Abbreviations	12
Chapter 1. Introduction	13
1.1. Introduction	13
1.2. Overview	13
1.3. Thesis Objectives	14
1.4. Research Contribution	14
1.5. Thesis Organization	14
Chapter 2. Background and Literature Review	16
2.1. Basics of Transceiver Design: Architecture, and blocks	16
2.2. LoRa Protocol Overview and its Applications	17
2.3. CubeSats Requirements and Standards	19
2.4. Launch Cost	19
2.5. Harness Optimization	20
2.6. SX1261/2 Transceiver	20
2.6.1. Power consideration	20
2.6.2. Thermal consideration	21
2.6.3. LoRa and LoRaWAN packet duration	21
2.6.4. SX1261/2 measurements	22
2.7. Related Work	23
2.7.1 CubeSat AIS receiver	23
2.7.2 S-band transceivers	24
2.7.3 UHF transceiver II	24

2.7.4	ISIS TXS high data rate s-band transmitter	25
2.7.5	ISIS UHF downlink/VHF uplink full duplex transceiver	25
2.7.6	TOTEM nanosatellite SDR platform	26
Chapter 3. Wireless Communication Standards		27
3.1	LTE Mobile	27
3.2	Narrow Band IoT (NB-IoT)	28
3.3	LoRa	29
3.4	Bluetooth	29
3.5	Zigbee Wireless Mesh Networking	30
3.6	Spresense (Sony Protocol)	31
3.7	Wireless Communication Standards Comparisons	32
Chapter 4. Methodology		34
4.1.	Problem Formulation	34
4.2.	Daughter board Overview	34
4.2.1.	Data interface	35
4.2.2.	Micro-controller unit	35
4.2.3.	Memory	35
4.2.4	RF	35
4.2.5	Oscillator	35
4.3.	Bill of Material	35
Chapter 5. Design and Simulation Results		37
5.1.	Transceiver Schematic Design	37
5.2.	Receiver Analysis and Results	38
5.3.	Transmitter Analysis and Results	45
5.4.	Antenna Analysis and Results	47
Chapter 6. Conclusion and Future Work		49

References	51
Vita	55

List of Figures

Figure 1-1: Architecture Overview	14
Figure 2-1: Typical Transceiver Block Diagram [3]	16
Figure 2-2: Power Consumption & Heat vs. Supply Volt & Power Mode [21]	21
Figure 2-3: LoRa Packet Format [21]	22
Figure 2-4: Crystal Oscillator Temperature Response [21]	22
Figure 3-1: Bluetooth Protocol Architecture [39]	30
Figure 4-1: Daughter Board Block Diagram	34
Figure 5-1: RF Schematic	37
Figure 5-2: Digital Schematic	38
Figure 5-3: Receiver Schematic Diagram	38
Figure 5-4: S-Parameter Result	39
Figure 5-5: LNA Schematic Design	39
Figure 5-6: Simulation Result	39
Figure 5-7: Harmonic Balance Simulation of Mixer Schematic Diagram	40
Figure 5-8: Simulation Result of Harmonic Balance	40
Figure 5-9: Schematic Diagram of LNA	41
Figure 5-10: Simulation Result	41
Figure 5-11: S-parameter Schematic Design	41
Figure 5-12: S-parameter simulation Result	42
Figure 5-13: Link Budget Analysis Schematic Diagram	42
Figure 5-14: Link budget Analysis Simulation Result	43
Figure 5-15: Harmonic Balance Simulations Schematic Diagram	43
Figure 5-16: Harmonic Balance Simulation Result	44
Figure 5-17: S-parameter Simulation Schematic Diagram	44
Figure 5-18: S-parameters Simulation Result	44
Figure 5-19: S-parameter Simulation of Transmitter Schematic Diagram	45
Figure 5-20: Simulation Result for S-Parameters	45
Figure 5-21: Link Budget Analysis Schematic Diagram	46
Figure 5-22: Harmonic Balance Simulations Schematic Diagram	46
Figure 5-23: Simulation Result	47
Figure 5-24: Simulation Results	47

Figure 5-25: Antenna Design in HFSS	47
Figure 5-26: S-Parameters Simulation Result	48
Figure 5-27: VSWR	48
Figure 5-28: 3D Radiation Pattern of The Designed Antenna	48

List of Tables

Table 1-1: Launch estimated spacecraft cost per Kg [2]	13
Table 3-1: Wireless Communication Standards Comparison	32
Table 4-1: Component's name, footprint, and quantity used	35

List of Abbreviations

BoM	Bill of Material
I2C	Inter-Integrated Circuit
KG	Kilo Grams
LAN	Local Area Network
LEO	Low Earth Orbit
LoRa	Long Range
LPWAN	Low Power Wide Area Network
MCU	Micro Controller Unit
PCB	Printed Circuit Board
RF	Radio Frequency

Chapter 1. Introduction

1.1. Introduction

In this chapter, we provide a short introduction about the small satellite mass requirement and the encountered problems in this field. Then, we present the problem investigated in this study as well as the thesis contribution. Finally, general organization of the thesis is presented.

1.2. Overview

Space solutions are getting more complex by day with the high demand on the different applications needed. Spacecraft's mass can range from 100 gram to 1000 of Kgs [19]. Each spacecraft has different mass depends on the payload chosen and the application of it. With that being said, the harness of the spacecraft contributes to this total mass of approximately 20%. Many developers are trying to optimize the design of the spacecraft harness to contribute less to the total mass [1].

Optimizing the harness is still not enough to take its mass to zero. Launchers mass requirements are very strict and expensive. Table 1-1 shows the prices of some launchers per Kg for LEO applications.

Table 1-1: Launch Estimated Spacecraft Cost Per Kg [2]

Launch Vehicle	Payload cost per kg
Vanguard	\$1,000,000
Space Shuttle	\$54,500
Electron	\$19,039
Ariane 5G	\$9,167
Long March 3B	\$4,412
Falcon 9	\$2,720

This leads to limiting many institutions from developing space solutions due to the high price. In order to make space solutions more reachable to everyone, the mass needs to be reduced in order to lower the price of the launch. One of the subsystems in a spacecraft that contributes to the mass is the harness which we can reduce as much as possible by making the data transfer wirelessly between the systems [8].

Transceiver PCB is being addressed in Chapter 4 along with the detailed BoM used in Altium tool to design the schematic and layout. Chapter 5 presents the analysis performed on the transceiver using ADS to show the RF analysis. Finally, Chapter 6 concludes the thesis and outlines the future work.

Chapter 2. Background and Literature Review

In this chapter, we discuss the fundamentals of transceivers and the definitions of its blocks within the scheme of LoRa protocol and its applications. Then, we present the standards and constraints of building and launching any CubeSats. Finally, we discuss the related work in this field of research.

2.1. Basics of Transceiver Design: Architecture, and blocks

Most of the typical transceiver are made of the below block diagram. Depends on the type of communication and the frequency used, the transceiver architectures will differ.

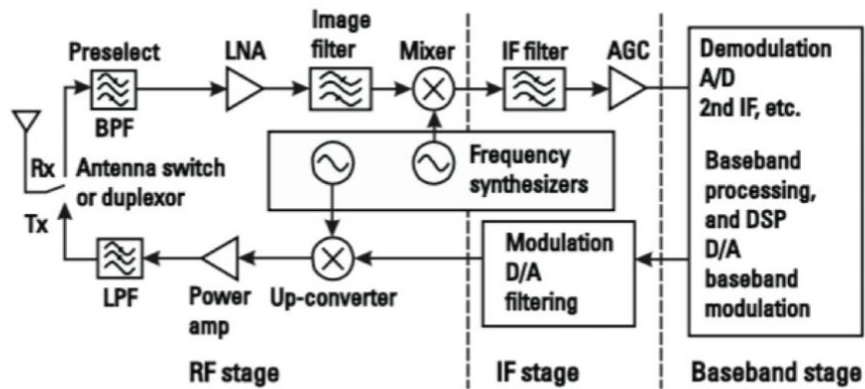


Figure 2-1: Typical Transceiver Block Diagram [3]

In Figure 2-1, the transceiver there are two sides, the first one is for receiving the signal and the other side is to transmit the signal. Both are sharing the antenna through a duplexer in order to switch between the two paths. At the receiver side, the first block faced by the incoming signal is the band pass filter (BPF) that is responsible for removing all the unwanted signals outside the designed band. After extracting the wanted signal, the Low Noise Amplifier (LNA) amplifies the signal with minimum noise added (the amount of noise depends on the chosen LNA) and pass it to another filter to remove the image signal. To verify the linearity of the device a measurement called Third-order input intercept point (IIP3) is considered in order to verify the RF performance. This measurement can be represented using the following formula:

$$IIP_3(dBm) = P_{in}(dBm) + \frac{\Delta P_{IMD3}}{2}, \quad \Delta P_{IMD3} \text{ is } IMD3 \text{ Power, } P_{in} \text{ is power in (1)}$$

The signal with minimum noise then enters the mixer in order to cover it from high frequency signal to intermediate frequency signal. This mixer has another input to it

which is the Local oscillator controlled by the voltage-controlled oscillator (VCO) inside the frequency synthesizer. The intermediate frequency wanted signal is the results of the difference between these two inputs.

At the Intermediate stage, there is another filtering block to remove unwanted signals before passing through the Automatic Gain control (AGC) [20]. This block is there to amplify the signal to the wanted baseband amplitude before digitalizing it and converting it to bits. A parameter that is commonly used to characterize a system front-end noise performance is the noise Figure (NF). It is the system signal-to-noise ratio at the input over the signal-to-noise ratio at the output as defined in the formula below:

$$NF_{dB} = \left(\frac{S_i}{N_i}\right)_{dB} - \left(\frac{S_o}{N_o}\right)_{dB} \quad (2)$$

On the transmitter side of the transceiver, the baseband signal enters the modulation block in order to modulate the carrier. Depends on the design of the transceiver, at the IF stage there is a filtering circuits to remove the noise around our signal that was generated at the Baseband stage. This helps reduce the output phase noise. Then comes the Upconverter which is responsible for converting the IF carrier and the Modulated signal into the RF frequency wanted signal. The other input of the mixer is from the frequency synthesizer. The resulting signal from the mixer then gets amplified by the Power Amplifier block to a certain level depending on the application we are using the transceiver for. Due to the amplification of the signal, some harmonics might be introduced due to nonlinearities, which needs to be removed by a lowpass filter [9].

2.2. LoRa Protocol Overview and its Applications

LoRa is the Physical layer used for Long Range communication application with high Data rate. LoRa modulation scheme is Chirp spread spectrum, which support low power characteristics like the Frequency Shift Keying but instead with higher communication range. This type of modulation has been used heavily in military and space communication due to its advantages: LPWAN has advantage on the low power consumption, which results in high battery lifetime compared to LAN and Cellular Network. Another thing is the low cost of implementing LPWAN network. The coverage of LPWAN is quite High which allows moderate amount of Data thru put [4]. There are so many applications that are utilizing these technologies ranging from health, agricultural, wireless sensor networks, traffic monitoring[5]. The creation of the low power, wide area networks (LPWANS) which have been developed through the LoRa

technology is required for the machine-to-machine and internet of things (IOT) applications:

- Traffic light management: LoRa is a sensor-based technology which coordinates its operation. The sensors get the input data and send them to the gateway to the main server. In the traffic, light management sensors are incorporated with the LoRa module. They detect the working of the traffic lights in time. In case there is a need to change or manage the traffic, LoRa sends a real-time message to the administration department.
- Autonomous vehicles: In this LoRa technology incorporated in the vehicle. They can drive automatically, and the distance is maintained. The technology also helps equip the vehicle with anti-theft function.
- Public illumination: LED bubbles are used for the illumination and can reduce energy waste by their application. LoRa technology is used to manage the illumination by changing bubbles and informing the management in case of anything.
- Energy resource and pollution measurement: the sensors can be used to issue the relevant local pollution index. The sensors can be used to make a follow up of the energy resources waste in the power plant.
- Intelligent delivery and inventory management: sensors with LoRa technology are being employed in warehouse management systems. sensors can send messages to the vehicle location and inventory situation regularly. This way the intelligence delivery and inventory management are catered for.

LoRaWAN has a couple of applications but most importantly to note is, it is used in cases with communication asymmetry. Due to the differencing volumes of data in the upper link and the downlink, in most cases used in the deployment of a wireless sensor network. This technology has found many applications into the different fields just like those discussed above. It is also used on the internet of medical things (IoMT). LoRa is also used in the agriculture for monitoring since it has a low-power utilization technique which enables long battery lifespan. it is used mostly in the end nodes distributed in the wide range fields. Another interesting aspect which will create more application for LoRaWAN is the localization and the tracking domains [5].

2.3. CubeSats Requirements and Standards

The fundamental unit for any CubeSat, the 1U has measurements of 10cmX10cmX10cm. CubeSats are exceptionally little satellites planned to carry smaller than expected payloads. Because of this small size, this introduces some challenges for the Satellite developers. Those challenges are Limited power generation, weight of less than 1 KG, and unified PCB dimension [6].

Most of CubeSat PCB design are based on PC/104 Specification. This standard is based on the 104 signal contacts on the two-bus connector of 64 pins on P1 and 40 pins on P2 [7]. This allows the stacking of the different PCBs in the structure much easier. There are certain requirements on the electrical and mechanical design of the CubeSat the following are the major ones [16]:

- Electrical Specification
 - Contact Resistance: <30 Milliohms Max
 - Current Capacity: 1 Amp continuous per pin
 - Dielectric strength: 1000 Vac
 - Insulation Resistance: 5000 Megohms Minimum
- Mechanical Specification
 - Housing: High Temp Thermoplastic
 - Contact: Phosphor Bronze
 - Solder: Tin-Lead (63-37)
 - Slower Clip: Aluminium Alloy

2.4. Launch Cost

Launch price is the main issue of space industry. In order to decrease the launch costs, there is generally a fixation with reducing system mass [12]. Launch Vehicles companies have so many containers and drivers for their designs such as payload comfort, mission flexibility and, launch cost. A further cost cut can be achieved however, that would impose some design change to the architecture and system design, which might impose some risks to the success rate of the launch [13].

The market of CubeSat is growing rapidly due to the ease of accessibility. This enables different types of missions that used to be hard in smaller platform [14]. For that reason, the launch market started to aim for the same shift that is happening with cubist

development to be applied to the lunch designs which should result in lowering the cost and complexity [15].

2.5. Harness Optimization

Harness is an essential subsystem in any spacecraft, designers in space projects are using different techniques for routing and manufacturing to optimize the design as much as possible. Many developers are focusing on the shielding of the harness to reduce the contributed mass from it [10]. Each mission designed differently which results in different harness routing depends on the complexity of it. This leads to growth of the harness routing which results in increasing the mass [11].

2.6. SX1261/2 Transceiver

These transceivers for radio frequency signals target the long-range and the wireless application of radio waves in GHz. SX1261 and SX1262 support two main types of modulation: LoRa and GFSK modulation. SX1261 and SX1262 have the capacity to demonstrate a large radiofrequency signal output. For example, the SX1261 is capable of transmitting up to +15 dBm while the SX1262 can transmit up to +22 dBm. When the SX1261 and SX1262 transceiver chips transmit such a high radio frequency, the power tends to generate a lot of heat. This heat can be transferred to the crystal resonator in the devices via the PCB. When the application is made for the long packet durations, the heat transferred tends to generate a frequency drift that can lead to errors in the receiver. Therefore, it is imperative to take enough precautions when designing the PCB to avoid such problems [21].

2.6.1. Power consideration

Notably, when the SX1261 transceiver chip is connected with a DC-DC converter, it can deliver up to +15 dBm of the maximum power output. The recommended power for this performance is between 1.8 V to 3.7 V through an LDO power supply. When the SX1262 is connected to the same system through a battery supply, it can deliver up to +22 dBm. Considering the efficiency of the power amplifier impacts the power that is delivered, it is notable that a part of the power delivered is transformed into the radio frequency signal. However, the remaining part of the power is dissipated into the SX1261/2 die, propagated to the QFN24 package, or transferred to the PCB sequentially [21].

The power dissipation can be demonstrated in Figure 2-2, which shows how power is consumed by the system and the amount of heat dissipated. The values are considered and demonstrated for the maximum power output for both transceiver chip versions at 250C. The systems are made for different configurations for the power supply for the different voltage conditions, either the LDO or the DC-DC configuration.

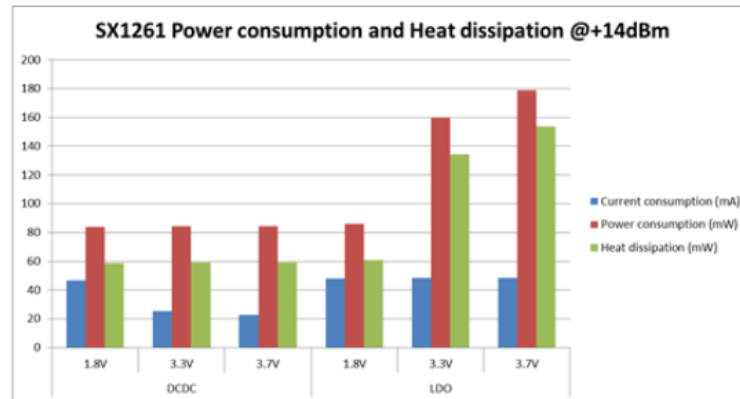


Figure 2-2: Power Consumption & Heat vs. Supply Volt & Power Mode [21]

Figure 2-2 demonstrates the benefits of using a DC-DC converter as it allows the power to be divided by half when compared to the LDO configuration. In addition, when the system configuration is maintained as this, the heat that is dissipated can be maintained at a constant level. However, when the LDO configuration is used, it is imperative to keep the input voltage as low as possible in order to minimize the power consumption and hence reduce heat dissipation [21].

2.6.2. Thermal consideration

In the process of transmitting a radio frequency, the heat that is generated in the SX1261/2 transmitter chip is transferred to the PCB. When the transmission takes a considerable long time, it ends up heating the crystal oscillator, making the frequency produced shift. When this shift happens, it leads to a deviation of the SX1261/2 RF. This deviation is a disadvantage to the performance of the system. It is important to minimize this deviation to ensure the optimal performance and reception of the packets. Depending on the constraints of the PCB device, such as its dimensions, the number of layers, and the position of the crystal oscillator, there may exist a trade-off between the Spreading Factor and the Bandwidth [21].

2.6.3. LoRa and LoRaWAN packet duration

A LoRa packet duration structure is shown in Figure 2-3.

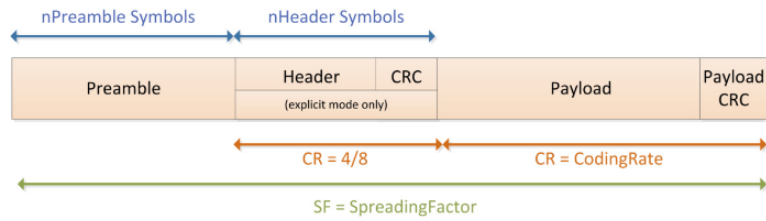


Figure 2-3: LoRa Packet Format [21]

In the LoraWAN specification, the system entails 3 fields: the MAC Header, the MAC Payload, and the MIC, which are 1 Byte, M Bytes, and 4 Bytes, respectively. In this system, it is imperative to use a low data rate optimization (LDRO) feature. This is imperative, especially when the time is beyond 16.38 ms, which should correspond to the SF11 and SF12 data rates. The use of the LDRO is important as it optimizes the reception of the packet even in situations where a long packet could provoke a carrier frequency deviation due to the heat dissipated by the PCB heating mechanism [21].

2.6.4. SX1261/2 measurements

To ensure efficiency in the transceiver transmissions, it is essential to measure the critical parameters in order to set them on the appropriate range. One of the important parameters for this system is frequency drift. The frequency drift for the SX1261/2 is measured based on the Semtech reference design of the PCBs at a frequency of 915 MHz Unless otherwise specified, the oscillator that is used in this system design measurement is the NDK NX2016SA. A sample illustration is made below to illustrate the different conditions for the voltage and the various configurations of the PCB [21].

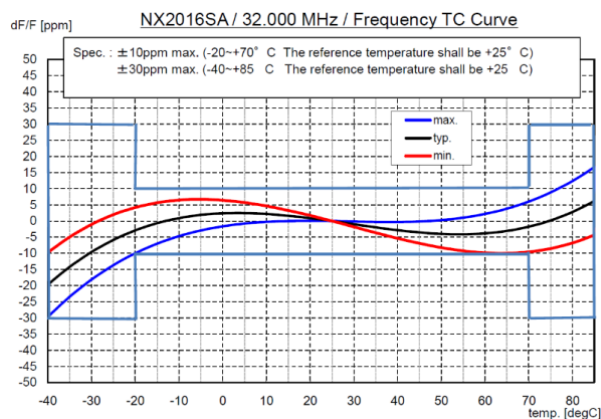


Figure 2-4: Crystal Oscillator Temperature Response [21]

As demonstrated in Figure 2-4 above, the behavior at 25°C shows that the crystal drops when the temperature increases. This means that when the SX1261/2 is subjected to a

long RF transmission, RF carrier frequency tends to drop. As this happens, a lot of heat tends to be generated and transferred to the PCB system and then to the crystal oscillator. The observations at 0°C and 50°C show that when there is a temperature variation, the crystal frequency response remains flat, which demonstrates no change. Therefore, variations can be measured within the temperature differences to note the highest chance for the highest frequency drift. The diagram above shows that the extreme temperature below -20°C and above 70°C creates even a higher frequency drift. It is important to handle these systems with care depending on the application scenario and the parameters used as the size of the PCB, the input voltage, the output power, and the duration of the packet [21].

2.7. Related Work

The communication links in a CubeSat necessitate low cost, low power, and small size transceivers. Furthermore, the link parameters associated with the satellite's operational environment can compromise mission data throughput. Thus, the choice of transceiver communication boards is integral to optimum CubeSat functionality. In each application case, the ideal communication board must have an appropriate mass, size, and radio frequency (RF) range. Moreover, the data throughput must be as high as possible, and a suitable transceiver must be used. The commonly available transceivers include AD9361, AD9364, CC1101, ADF7021, TH7122, and CC1120. These units are used to build several transceiver communication boards. The most notable products are the CubeSat AIS transceiver, S-band transceivers, the UHF transceiver II, the ISIS high data-rate S-band transmitter, the ISIS VHF uplink/UHF downlink transceiver, and the TOTEM nanosatellite SDR platform. The below review will essentially compare these systems to provide precedence for selection in different scenarios.

2.7.1 CubeSat AIS receiver

The CubeSat AIS is a compact unit developed primarily to receive signals. It is entirely software-based, self-contained, and customized for the maritime VHF band [22]. The system also comprises demodulators for receiving conventional and long-range AIS communications. Furthermore, it provides excellent performance, considering CubeSat's power, weight, and size constraints. The AIS system can also offer additional payloads on bigger LEO satellites. The unit measures 93.0 mm by 87.2 mm by 12.45 mm [22]. Moreover, the overall weight is 185 g [22]. The frequency coverage is

between 156.000 MHz to 162.025 MHz [22]. The system also operates in four AIS channel frequencies: 162.025 MHz, 161.975 MHz, 156.825 MHz, and 156.775 MHz [22]. Despite having a high performance, this unit must be combined with a separate AIS transmitter. Thus, the volume and mass may increase.

2.7.2 S-band transceivers

S-band transceivers are diverse, and their specifications vary. The CubeSat S-band transceiver designed by Nano Avionics is among the most reliable alternatives. This system is essentially a low-power full-duplex transceiver uniquely suited for nano and micro-satellites. It functions on S-band frequencies with CCSDS recommended channel coding and GMSK modulation. Thus, it can be easily integrated with commercial and private ground stations. The transceiver also has filtered RF connections for output and input, accommodating separate transmitting and receiving antennas. The transmit frequency ranges from 2200 MHz to 2290 MHz, and the transmit bit rate is between 100 kbps and 500 kbps [23]. Contrarily, the receive frequency ranges from 2025 Hz to 2110 MHz at a 100 kbps bit rate [23]. The transceiver measures 93.0 mm by 87.2 mm by 17.0 mm and weighs 191 g [23]. The S-band transceiver is superior to the AIS alternatives.

The S-band transceiver I is also highly efficient in CubeSat applications. It is uniquely designed to facilitate secure telecommands and telemetry. The unit also has configurable data rates to facilitate in-orbit update applications. Moreover, it employs the Advanced Encryption Standard (AES)-128/256 to offer optimized security [24]. Thus, the best-suited applications are in-orbit updates, telecommunications uplink, and inter-satellite communications. The transceiver is also suited for the industrial, scientific, and medical (ISM) and commercial bands. Specifically, the commercial frequency range is 2200 MHz to 2290 MHz and 2025 MHz to 2110 MHz [24]. Conversely, the ISM range is 2400 MHz to 2450 MHz for both Tx and Rx [24]. The transceiver weighs 200 g, and it measures 95.9 mm by 90.2 mm by 23.3 mm [24]. These specifications qualify the unit for both CubeSat and nanosatellite LEO applications.

2.7.3 UHF transceiver II

The UHF transceiver II is a half-duplex communication system suited for LEO applications. It accommodates output power customization and various modulation methodologies for telecommand and telemetry. The unit's data rates are also

configurable, facilitating changes while the CubeSat is still in orbit. Moreover, the transceiver communication board is encapsulated in an aluminum containment specifically designed to block particle radiation, reduce EMC, and dissipate the power amplifier's heat. The transceiver's RF range is 430 MHz to 440 MHz and 400 MHz to 403 MHz [25]. Furthermore, the entire ensemble weighs 90g and measures 89 mm by 95 mm by 23.2 mm [25]. These specifications allow the unit to fit in a CubeSat, but a second similar transceiver can be incorporated into the ground station.

2.7.4 ISIS TXS high data rate s-band transmitter

The ISIS high data-rate S-band transmitter is specifically designed to provide fast communication. It gives data rate downlinks reaching 4.3 Mbps, suiting it for the information bit-rate at the CCSDS transfer frame level. Notwithstanding, the communication board can be used for PDT and TT&C downlinks. The system is also highly flexible, employing CCSDS as the data link layer framework and accommodating in-orbit alteration of the RF output power frequency, modulation scheme, and data rate. The frequency ranges between 2200 MHz and 2290 MHz with a 1 kHz step size [26]. Furthermore, the transmitter weighs 120 g and measures 98.81 mm by 93.26 mm by 14.52 mm [26]. Despite its superiority regarding data rate, this unit must be combined with a corresponding receiver. This process increases the mass and volume. Nonetheless, the system still meets CubeSat standards.

2.7.5 ISIS UHF downlink/VHF uplink full duplex transceiver

The ISIS VHF uplink/UHF downlink transceiver is an appropriate substitute to the ISIS high data-rate S-band transmitter. It is essentially a full duplex communication board for CubeSat applications. Furthermore, it can function in amateur and commercial bands in the UHF and VHF frequency spectrum. The system is highly configurable, low mass, and low power. It also accommodates in-orbit configuration of data rates, accentuating its flexibility. Unlike many other alternatives, the ISIS VHF uplink/UHF downlink transceiver is cross-compatible with different subunits, such as antennas. The transceiver is not contained by shields, and it measures 90 mm by 96 mm by 15 mm [27]. Moreover, the system weighs 75 g and operates in two main RF ranges: 400.15 MHz to 402 MHz and 435 MHz to 438 MHz [27]. However, other RF ranges are available on request to the manufacturer.

2.7.6 TOTEM nanosatellite SDR platform

The TOTEM nanosatellite SDR platform is a high-performance communication board for nanosatellites with a UHF front end. It also meets the CubeSat standards. The TOTEM motherboard serves as the transceiver and control unit. Contrarily, a piggyback board provides the external UHF front end. The system has a wide frequency range and an embedded Linux, covering virtually all critical nanosatellite RF bands and allowing the rapid deployment of several SDR applications simultaneously. The UHF and SDR front end component feature 5 W at 30 dBm in 437MHz [28]. Furthermore, the SDR is configurable from 70 MHz to 6 GHz [28]. Like the ISIS communication boards, the TOTEM nanosatellite SDR platform is not covered in an elaborate compartment. The panel measures 89.3 mm by 93.3 mm by 13.9 mm and weighs 131 g [28]. The TOTEM nanosatellite SDR platform is preferred due to its additional roles other than sending and receiving communication.

Chapter 3. Wireless Communication Standards

Various wireless communication standards available in the market characterize features specific to a product range, with their data range, range and coverage, applications, power consumption, battery life, cost, and frequency tailored to specific needs. In particular, their development was geared to solve shortcomings and gaps in the technological field, which necessitates an in-depth overview and comparison to determine their usability in various niches according to their specifications. Hence, the current study seeks to compare LTE Mobile, Narrow band IoT, LoRa, Bluetooth, Zigbee, and Spresense (Sony protocol) wireless communication standards and features. While the researched wireless standards seek to improve on existing and earlier communication standards' limitations in various niches, they contain delimiting factors that makes them suitable only for serving specific technological needs meaning that no single protocol achieves universal applicability.

3.1 LTE Mobile

LTE, an acronym for Long-Term Evolution standard, compose a data terminals and mobile devices standards' wireless broadband communication that uses packet switching, and it is based on UMTS/HSPA and GSM/EDGE standards [37]. The evolution of mobile communication standard from GSM, UMTS, HSPA or CDMA to LTE enables for a significantly more improved speed and capacity [32]. While the standard generated MTS standards, the technology comprises new standards that enabled for increased upstream and downstream peak data rates, all IP network, upgraded spectral efficacy, scalable bandwidth, and multiuser support [32]. Hence, the LTE communication standards bridged the practical data exchange gap between mobile devices networks and fixed wireless LANs (Local Area Networks) [32]. The LTE project, initiated by the European Telecommunications Standards Institute (ETSI) and other actors, sought to craft a standard that maintained competitiveness in the coming decade regarding data transfer efficiency through the simplification and optimization of radio access network (UTRAN) and the augmentation of the radio access technology (UTRA).The primary driving factors comprises greater data transfer at lower latency rates, effectual spectrum utilization, reduced operation cost, flexible spectrum distribution, and enhanced system coverage and capacity [32]. As such, the 3GPP TR 25.913 (LTE) standards targets include:

- Lower latency rates
- Increased cell bit rate performance
- Enhanced spectral efficiency: 2.5 and 5 bps/Hz for UL and DL respectively.
- Enhanced peak data rate: 50 and 100 Mbps for 20 MHz UL and 20 MHz DL (with 2Rx antenna) [32].

3.2 Narrow Band IoT (NB-IoT)

NB-IoT composes a LPWAN (low power wide area network) radio technology standard for mobile services and devices. It enables for a wide variety of IOT-related systems, with its use allowing for spectrum and system capacity efficiency, and low power consumption, long battery life, increased indoor coverage, secure connectivity, simplified network deployment and topography and high connectivity density [33]. NB-IoT, a project by 3GPP, uses an LTE standard subset but limits the bandwidth to 200 kHz bandwidth [33]. In its licensed spectrum, Narrow Band IoT characterizes no duty cycle limitations, while using SC-FDMA (Single-carrier FDMA) for uplink and OFDM (orthogonal frequency-division multiplexing) for downlink communication [36].

There composes several similarities and differences between NB-IoT and LTE. For instance, the following specs are similar to both communication standards:

- 1ms subframe length
- 10 subframes at 10ms in a Radio Frame
- 2 slots in a subframe
- 15Khz subcarrier spacing
- OFDMA downlink waveform [36].

Similarly, NB-IoT introduced some notable changes from LTE standards, namely:

- 200kHz fixed system bandwidth for NB-IoT.
- Use of SC-FDM waveform for uplink communication
- SSS and PSS transmission pattern and resource element mapping
- Use of three types of DCI format (N0, N1, and N2)

Performance of repetitive transmission on almost all channels, while LTE uses TTI Bundling for repetitively transmission and reserves all others for single transmission [36].

3.3 LoRa

LoRa, an RF wireless modulation technique and physical layer technology based on CSS (chirped spread spectrum) and works based on sub-GHZ ISM band [30]. The name references the long range data transfer capabilities for LPWANs (low-power, wide area networks) [40]. LoRa characterizes ultra-low power usage coupled with an open LoRaWAN, topology protocol usable for low power requirements, small data usage, long range, low cost, constant roaming, and deep in-spaces communication devices [140]. The wireless communication protocol uses single-hop technology that supports from 300bps to 50Kbps channel bandwidth settings -and spreading factor-dependent data transfer rate, and it relays data through gateways to the central servers [40]. Also, it allows multiple transmissions simultaneously with different spreading factors, and it includes LoRaWAN (long-range wide-area network) system architecture and communication protocol that includes upper layer and network functionality [40]. It also provisions various ISM frequencies in North America (915 MHz), Europe (868 MHz), and Asia (433MHz) [40]. LoRa has an advantageous position when the user needs an end-notes, transport-layer security, wide range deployments, and low power applications [34]. However, its lack of global outreach, low-data transmission rates, and country-specific data regulations limits its usage as a uniform global solution to communication [34].

3.4 Bluetooth

Bluetooth composes a short-range wireless communication protocol that is used to transfer data between cellular, mobile, or fixed devices using ISM bands and UHF radio waves. It uses a bandwidth of 2.40 to 2.48 GHz, with the range varying from 10 to 100 meters, a data transfer rate from 1-2 bit/s and a 0.3 ma power consumption rate [29]. However, in a one-on-one scenario, Bluetooth comprises a 723 kb/s data transfer speed [29]. It supports a point-to-point and point-to-multiple devices data transfer, with the former using a master and slave relation [29]. Its connection to a device creates a personal area network (PAN) that uses an independent stack of protocol model that deviates from the standard TCP/IP or OSI communication protocols used in wireless

data transfers [39]. The Bluetooth architecture protocol compose a physical layer (radio and baseband), data link layer (link manager protocol [LMP] and logical link control and adaptation protocol [L2CAP]), middleware layer (RFComm), adopted protocols, and service discovery protocol [SDP]), and an application layer as shown in Figure 3-1.

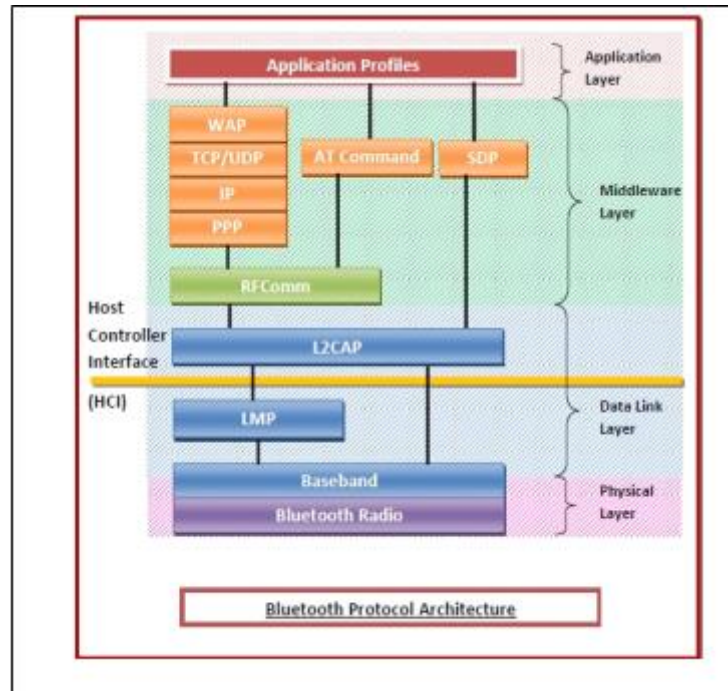


Figure 3-1: Bluetooth Protocol Architecture [39]

Bluetooth offers some advantageous characteristics features that set itself apart from other wireless communication protocols. For instance:

- It offers a low cost wireless solution at relatively short distances
- Inbuilt device which requires no setup files
- Global specification usage
- Connection supports up to 8 different devices
- Omnidirectional signal output
- Signals transmission over barriers such as walls [29].

3.5 Zigbee Wireless Mesh Networking

Zigbee composes an open global wireless communication protocol that seeks to fulfill a low cost, low power internet of things (IoT) networks, and it operates on a packet-based protocol using 868 MHz, 900 MHz, and 2.4 GHz bands using an IEEE 802.15.4

specifications [41]. It allows interoperability of devices from various manufacturers and its connection to an IP domain enables control from devices such as smartphones [41]. The Zigbee protocol characteristics include:

- Low latency
- Up to 65,000 nodes/ network
- High battery life due to low duty cycles
- Support for point-to-point, point-to-multipoint, and mesh networks
- DSSS (Direct Sequence Spread Spectrum)
- Secure data connections and 128-bit encryption
- Centralized and distributed security [41].
- Evenly distributed loads
- Scalable and flexible network structure [42].

Zigbee integrates a “base device” that provides consistent activities that commissions nodes into a network, with its architecture composing of a router, coordinator, and an end device [41]. In particular, Zigbee architecture uses an IEEE 802.15.4 protocol that incorporates several layers including the physical layer, MAC layer, network layer, application support sub-layer, and application framework [42]. Zigbee uses various network topologies, with the most common being the cluster tree and star mesh topologies [42]. Due to its low power operating mode, small cost, and topologies, its features make it the most suitable method for several IoT-based applications over Wi-Fi and Bluetooth.

3.6 Spresense (Sony Protocol)

Spresense composes programmable communication modules that uses the CXD5602 and CXD5247 chips with six low power consumption processor cores that allows for connectivity capabilities [34]. It composes a GPS satellite antenna and a pin socket with I2C, SPI, I2S, AIN, and UART that enables an individual to add communication modules that would enhance IoT capabilities. Additionally, it includes multi-mic input and Hi-res audio output, multi-core controller, high precision positioning features, and extensive computing power [38]. Its main advantage composes low power consumption, while also incorporating flexibility in usage as a user can add several modules and program it for various tasks.

3.7 Wireless Communication Standards Comparisons

While the various communication protocols characterize improvements on earlier challenges based on upcoming challenges, their features provide specialized needs that provide solutions to niche technological and consumer needs, for instance, LTE mobile improves on earlier standards while maintaining long range, which reduces the associated operating costs. On the other hand, NB-IoT deviates somewhat from LTE mobile to provide a more specialized changes resulting in a higher battery lifetime and lower cost (making it suitable for smart IoT devices) but resulting in reducing range and coverage. LoRa characterizes a direct challenger to NB-IoT in providing IoT solutions, although its lack of uniform global solution to communication limits its applicability. For shorter ranges, Bluetooth offers a low cost simple solution to connection at short distances, although Zigbee wireless mesh networking provides more significant features such as increased nodes and security, albeit at a higher cost and power consumption rate. Finally, Spresense, the Sony protocol, provides specialized wireless communication protocols for hobbyists and users with specific needs, with its flexibility in adding modules and programming needs excluding most consumers. Therefore, the examined wireless protocols each provide specialized features that adequately covers various product niches. Table 3-1 summarize the discussed wireless standards with the main features: data rate, range and coverage, applications, power consumption, battery lifetime, cost, and frequency.

Table 3-1: Wireless Communication Standards Comparison

Wireless Standards	Data Rate	Range and Coverage	Applications	Power Consumption	Battery Lifetime	Cost	Frequency
LTE Mobile	<ul style="list-style-type: none"> • 5 and 12 Mbps (download) • 2 and 5 Mbps (upload) 	5-30 Kms	cellular network	3772.1 w	4.7 years	n/a	1850 MHz to 3800 MHz
Narrow band	<ul style="list-style-type: none"> • 26 (kbps) uplink peak data rates up to 62 kbps • (Single-carrier FDMA) for uplink and OFDM (orthogonal frequency-division 	1 Km (urban) 10Km (rural)	smart metering, IoT, and connected personal appliances	n/a	10 years	\$5 (starting price)	Geo-dependent: <ul style="list-style-type: none"> • North America (915 MHz), • Europe (868 MHz), • Asia (433MHz)
LoRa	100 Kbps for GFSK and 0.3 to	• 2- 5 kms (urban) •	Smart devices and IoT	2.25 w	1 year	\$2.56 (starting	863-870; 902-928; and

	22 Kbps for LoRa modulation	15 km (rural)				price)	779-787 MHz
Bluetooth	<ul style="list-style-type: none"> • EDR PHY (8DPSK): 3 Mb/s • EDR PHY ($\pi/4$ DQPSK): 2 Mb/s • BR PHY (GFSK): 1 Mb/s 	• 1-100 m (based on radio class) at 8-cell nodes	Point-to-point and point-to-multipoint communication between devices such as: cellular pc, and smart TV's	10 -30 mA	500 cycles	\$2.50	2.4 GHz – 2.483 GHz
Zigbee	<ul style="list-style-type: none"> • 250 kbps for 2450 frequency band) • 40Kbps for 915 frequency band • 20 kbps for 868 frequency band 	• 10-100 meters at 6500 cell nodes	Smart applications and IoT	10-100 Mw	10 years	\$0.10 per foot	2.4 GHz
Spresense (Sony Protocol)	n/a	n/a	Geo-locations, audio processing, and other variable uses	300mW	n/a	\$130.00	156 MHz

Chapter 4. Methodology

In this chapter, we define the high-cost problem of launching spacecrafts into space which is directly proportional to the weight of it. We also present the proposed PCB solution to reduce the weight contributed from the spacecraft harness.

4.1. Problem Formulation

We consider a mini modular transceiver PCB (Daughter board) that gets attached on top of any PCB within the CubeSat (Mother board) without inducing any changes. Those daughter boards will be responsible for sending and receiving all the data wirelessly between the subsystems instead of using the harnesses.

4.2. Daughter board Overview

The daughter board is responsible for collecting all data from the mother board using I2C then read by the MCU on it. The MCU will unpacketize the received data and then packetize it again and send it through SPI to the transceiver. This transceiver will then modulate using LoRa scheme and power amplify it then send it through the antenna on the board to be received to other daughter board. and vice versa for receiving. In order to avoid any possible cross talking between the different boards, class B for LoRa has been chosen which will have a bi-directional communication with a pre-defined time window for the transmit a receive data payload. Along with that, a time-synchronized bacon will be used in between the boards in order to synchronize between the subsystems within the CubeSat.

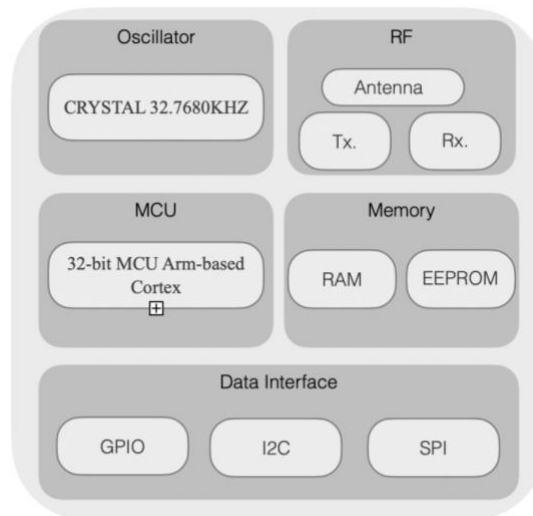


Figure 4-1: Daughter Board Block Diagram

Figure 4-1, shows the Daughter Board block diagram which consists of 5 major blocks as follow:

- 4.2.1. Data interface** It consists of three interfaces: GPIO, I2C, and SPI.
- 4.2.2. Micro-controller unit** It is a 32-bit Arm-Based Cortex
- 4.2.3. Memory** Internal memories of RAM and EEPROM are used for Data.
- 4.2.4 RF** The Radio Frequency block is the Transceiver and the antenna.
- 4.2.5 Oscillator** A 32.7680KHz oscillator to be the main clock supply as per the datasheet recommendation

4.3. Bill of Material

The below table 4-1 summarize the bill of materials used in the Altium schematic design. The table shows all the part number, footprint, and quantity used.

Table 4-1: Component's Name, Footprint, and Quantity Used

Comment	Footprint	Quantity
GRM033C81A105ME05D	FP-GRM033-0_09-IPC_C	2
C0402C220J8GACTU	FP-C0402-BB-MFG	2
GRM033C80G104KE19J	CAPC0603X33X15NL03T05	9
C0603C475K9PACTU	FP-C0603-CG-MFG	1
C0402C279D5GACTU	FP-C0402-BB-MFG	1
C0402C470K3GAC7867	FP-C0402-BB-MFG	2
C0402C689C5GACTU	FP-C0402-BB-MFG	4
CAP 4.7pF 50V 0402(1005)	CAPC0402(1005)60_N	3
GRM155R61E102KA01D	CAPC1005X55X25ML05T10	1
ANT-868-CHP-T	ANT-868-916-CHP	1
62201621121	62201621121	1
LQG15HS12NJ02D	INDC1005X55X25LL05T10_A	1
LQW15AN15NJ00D	MURA-LQW15A-0402_L	2
RK73B1JTTD472J	RESC1608X55X30ML20T10	2
RK73B1ETTP304J	RESC1005X40X25ML10T10	1
RN73H1ETTP1002B25	RESC1005X40X25ML10T10	1

RT0402BRD073K74L	FP-RT0402-MFG	1
RN731JTDD9651B10	FP-RN731J-IPC_C	1
SX1276IMLTRT	SMTC-QFN-28_V	1
AP7365-30YG-13	FP-SOT89-MFG	1
STM32L051K8U6	STM-UFQFPN32_L	1
SC4215ASTRT	SEMT-SOIC-8_V	1
4259-63	PERE-SC-70-6_M	1
WMRAG32K76CS1C00R0	OSC_WMRAG32K76CS1C00R0	1

Chapter 5. Design and Simulation Results

In this chapter, the daughter board schematic design is presented. The schematic is drawn using Altium Design tool with all the parts selected in the bill of materials. Along with that, we present the simulation design and results achieved for the transceiver implemented. We also present the antenna design and simulation. The LoRa transceiver has been designed for central frequency of 868MHz.

5.1. Transceiver Schematic Design

The schematic design contains all the parts to design the daughter board connected in between to perform the objectives. Figure 5-1 shows the ISM 868MHz embedded ceramic antenna connected to a high power UltraCMOS RF switch. This RF switch is controlled using 1 pin and it can accomplish a 1dB compression point of +33.5 dBm by using 3.0V supply.

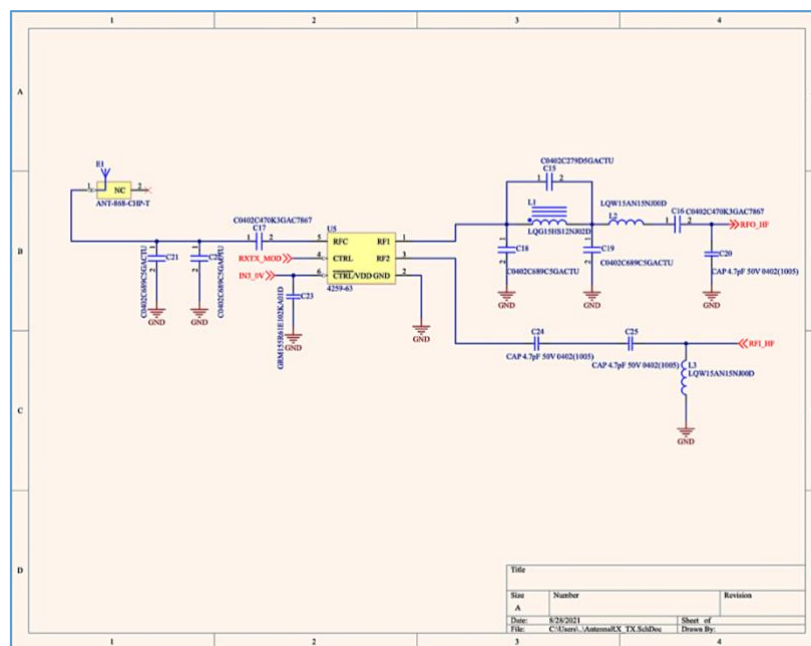


Figure 5-1: RF Schematic

The RF input/output signals are connected into the low power long range transceiver. This transceiver is a high sensitive down to -148 dBm with great immunity blocking. It provides multiple modulation scheme and the one used in the design is LoRa modulation. Figure 5-2 shows the transceiver connected to an ultra-low power 32bit microcontroller Arm based cortex. They are connected using 4 main signals: SPI clock

input, SPI data output, SPI data input, and SPI chip select input. This MCU is connected to a 32kHz resonator and voltage regulator to supply the needed voltages. This MCU is connected to headers to send and receive data using I2C bus.

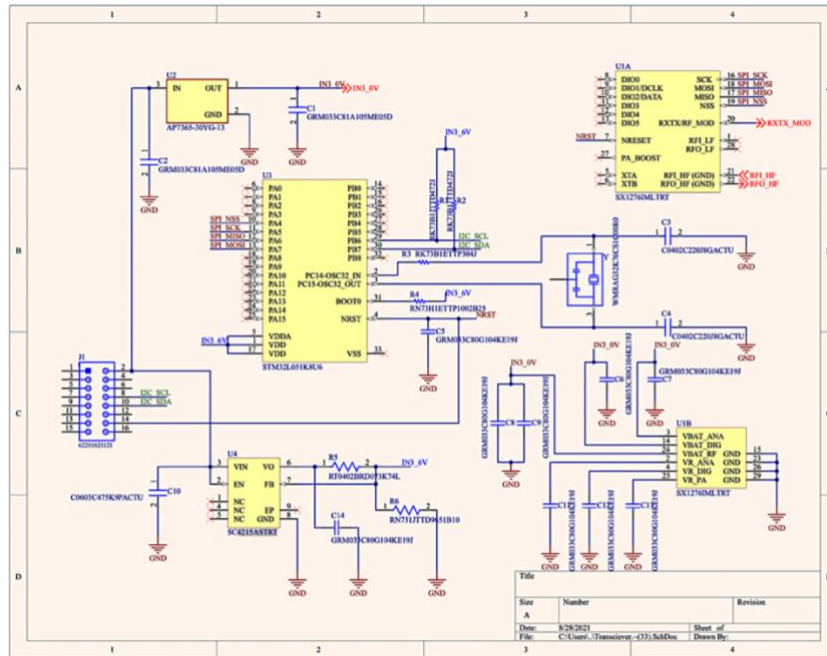


Figure 5-2: Digital Schematic

5.2. Receiver Analysis and Results

In the transceiver the receive chain consists of BPF, mixer and LNA which receives the signal of interest, then it gets down converted, and amplified. The schematic diagram of the receiver with the above-mentioned components is shown in Figure 5-3.

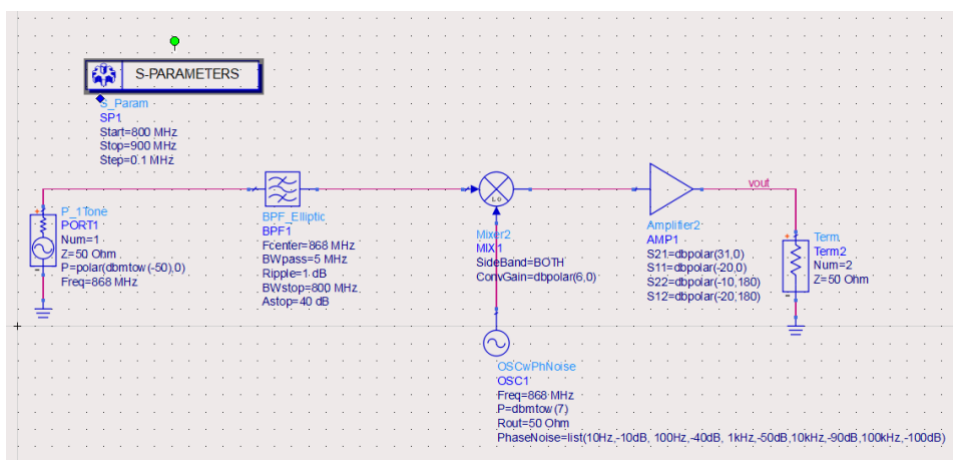


Figure 5-3: Receiver Schematic Diagram

The simulations result of s-parameters is shown in Figure 5-4.

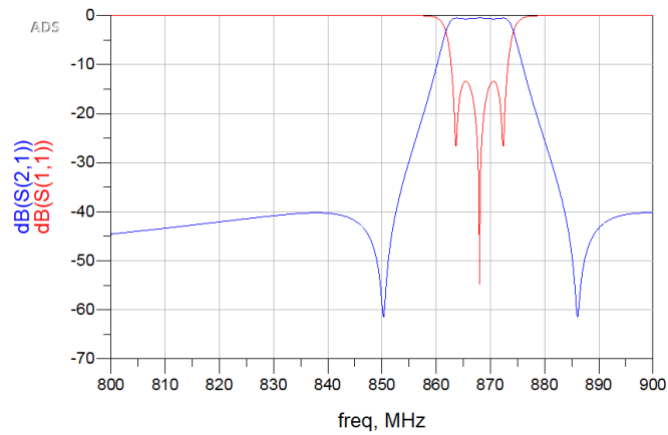


Figure 5-4: S-Parameter Result

The response of the LNA was also examined and the schematic for LNA is shown in Figure 5-5 and Figure 5-6. LNA input is coming from a pulse source of time period 100nS and pulse width of 30nS.

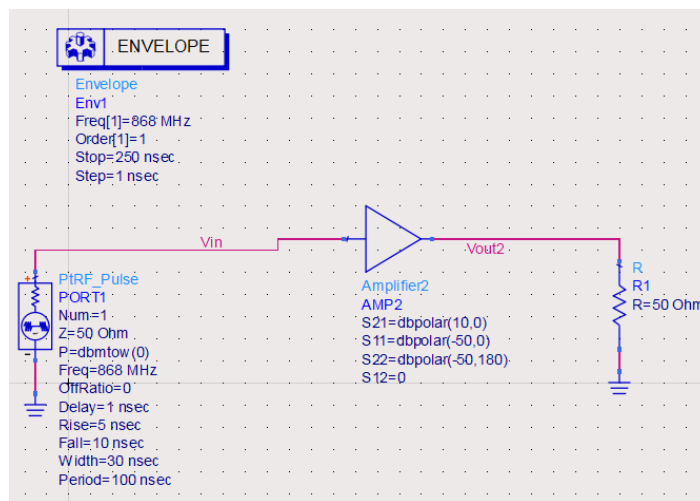


Figure 5-5: LNA Schematic Design

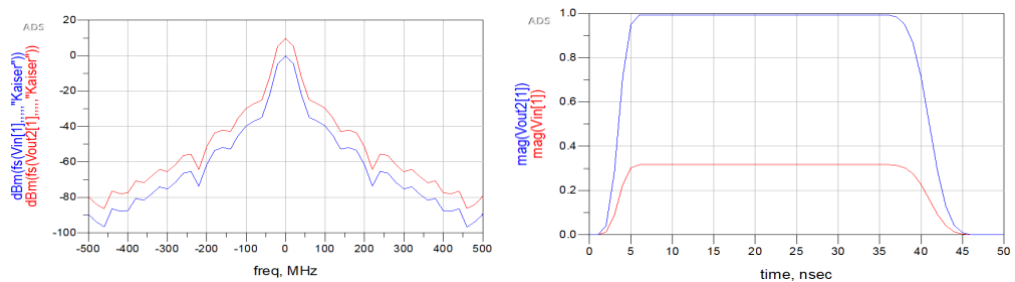


Figure 5-6: Simulation Result

To view the response of the mixer for frequency conversion, the schematic is shown in Figure 5-7. The input power is -50dBm and IF frequency is 70MHz and frequency of LO is 798MHz.

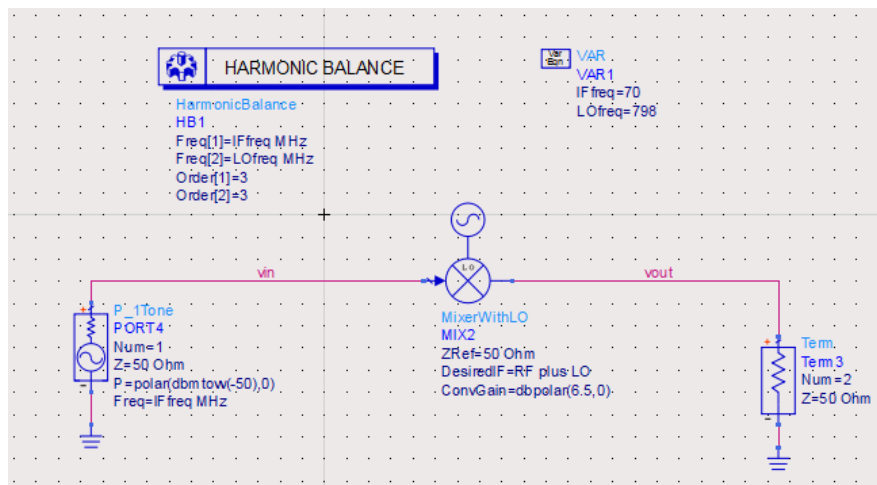


Figure 5-7: Harmonic Balance Simulation of Mixer Schematic Diagram

The result of harmonic balance simulations is shown in Figure 5-8. The input frequency signal is 70 MHz shown in the Figure with -47dBm signal level. After frequency conversion upper and lower band of mixed signal the signal shows an amplitude level of -43.5dBm at 728MHz and 868MHz. The signal of LO with frequency 798MHz is also appeared at output due to limitation of LO-RF isolation.

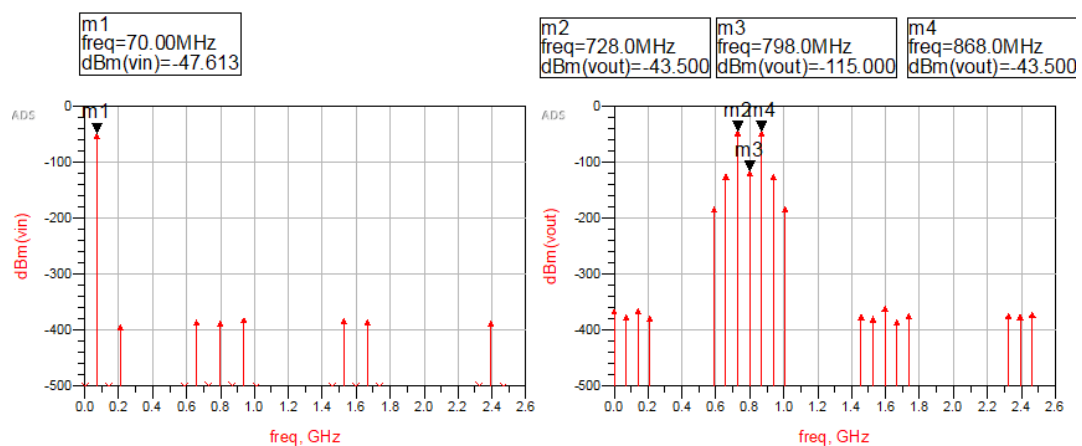


Figure 5-8: Simulation Result of Harmonic Balance

For the transmitter, power amplifier has also individually analyzed for operating frequency of 868MHz. The schematic for harmonic balance and gain compression simulations is shown in Figure 5-9 and Figure 5-10.

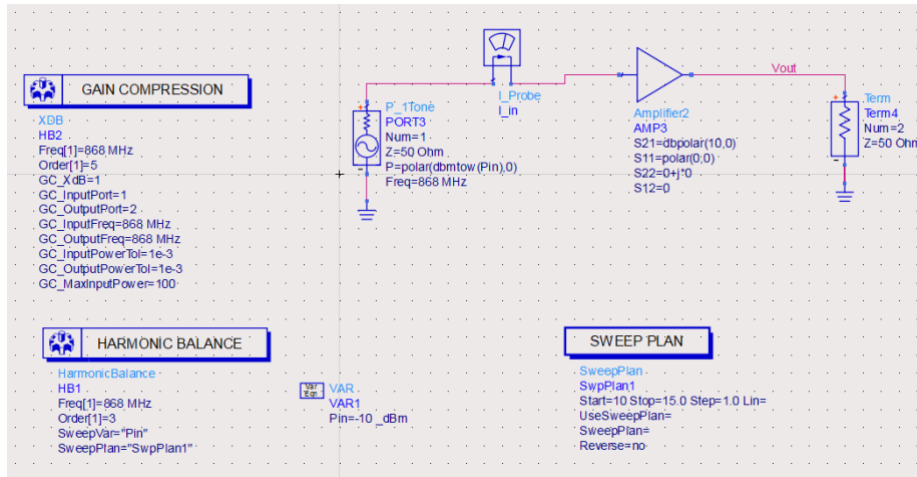


Figure 5-9: Schematic Diagram of LNA

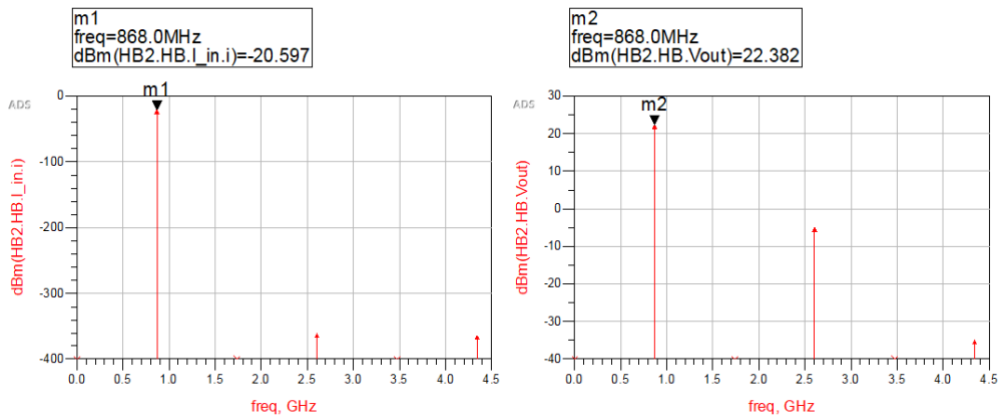


Figure 5-10: Simulation Result

For s-parameters simulations of receiver circuit the schematic is shown in Figure 5-11 and the result from the simulation is illustrated in Figure 5-12.

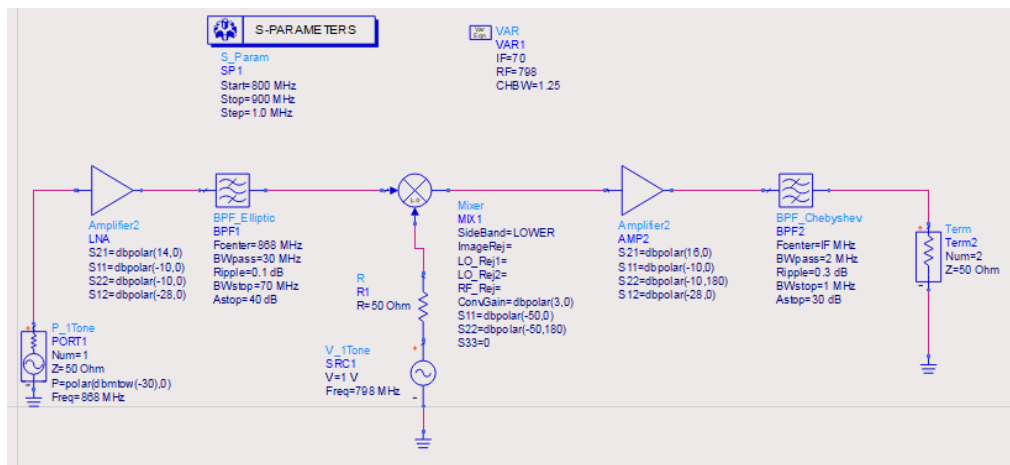


Figure 5-11: S-parameter Schematic Design

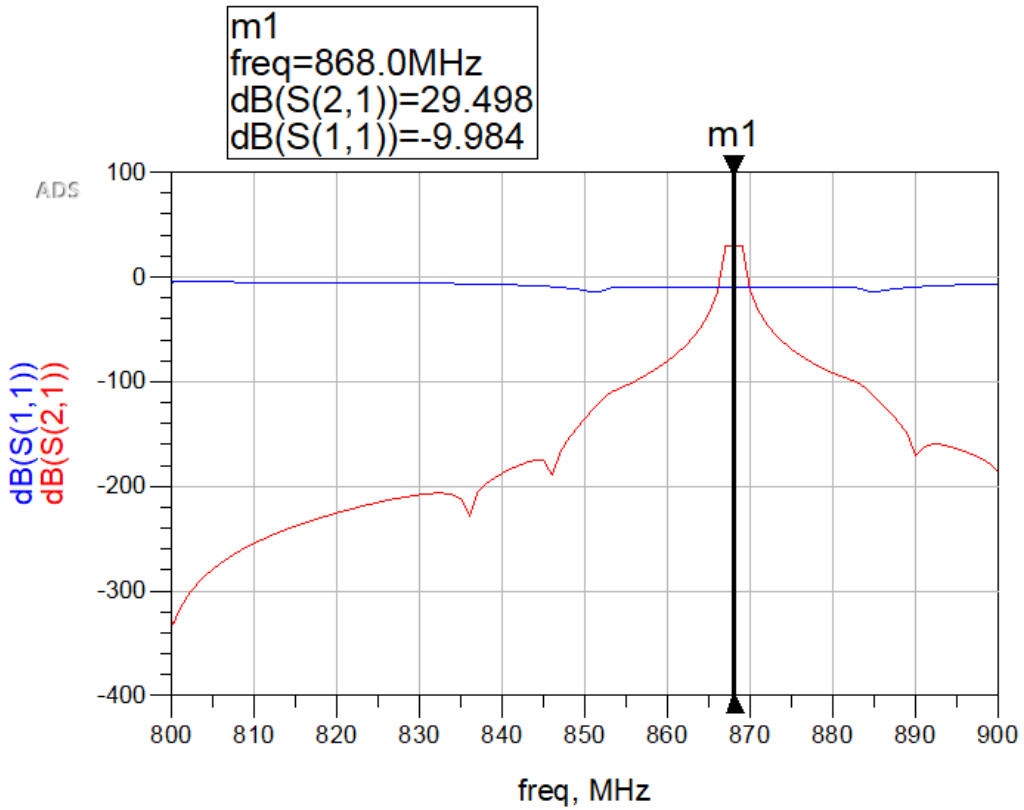


Figure 5-12: S-parameter simulation Result

The receiver schematic diagram for link budget simulation is shown in Figure 5-13 and the results are shown in Figure 5-14.

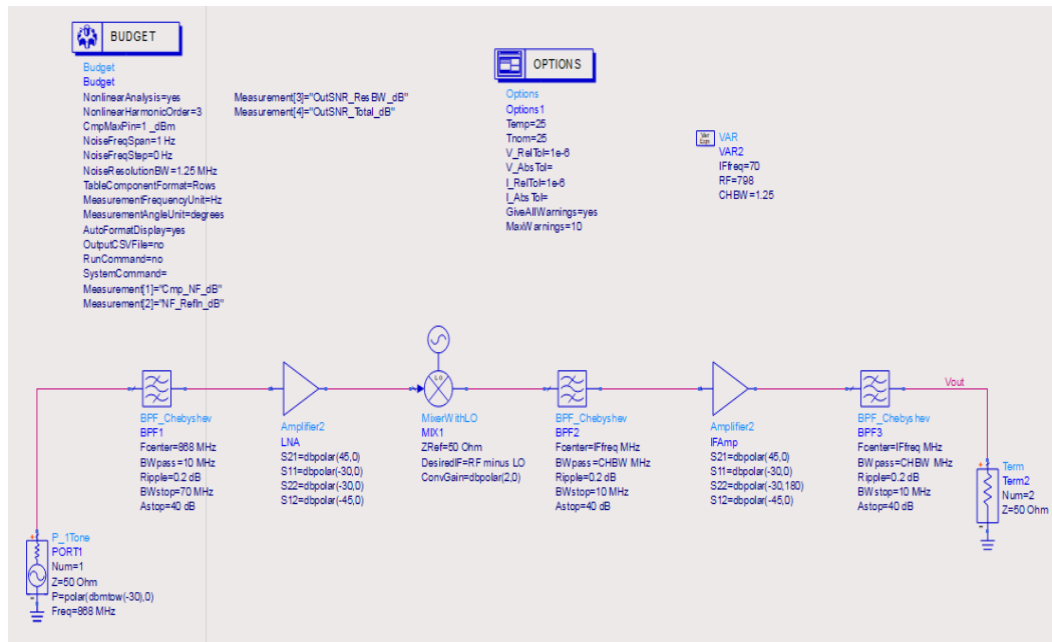


Figure 5-13: Link Budget Analysis Schematic Diagram

Cmp_RefDes	Cmp_NF_dB	NF_RefIn_dB	OutSNR_ResBW_dB	OutSNR_Total_dB
BPF1	0.300	0.300	82.614	143.583
LNA	1.902	2.200	80.570	141.539
MIX1	15.401	4.852	77.695	138.664
BPF2	0.400	4.852	77.695	138.664
IFAmp	3.002	4.853	73.349	134.318
BPF3	0.400	4.853	73.349	134.318

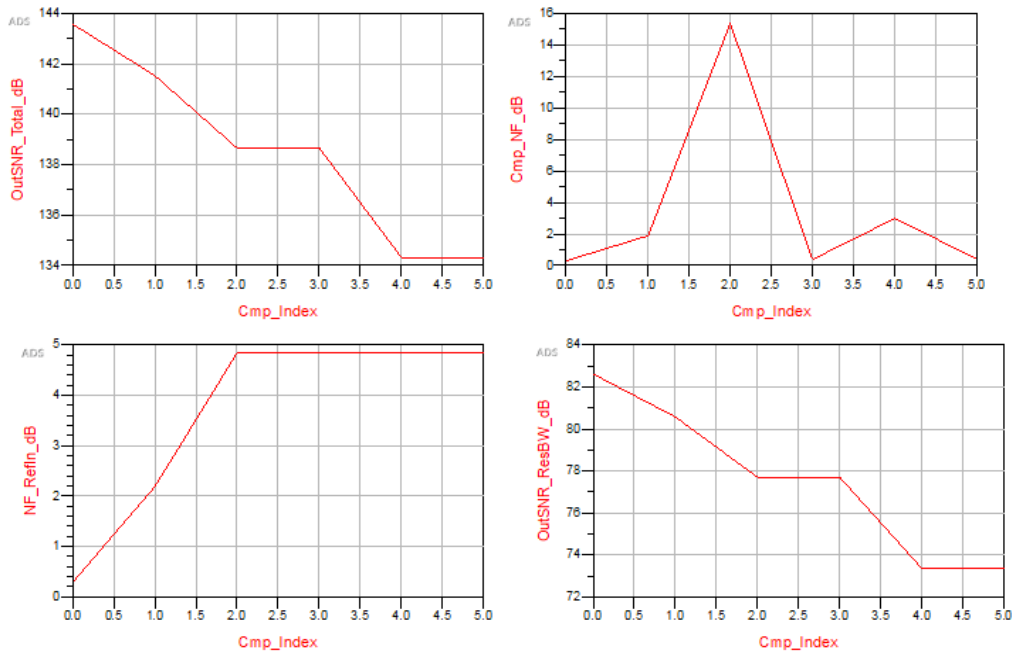


Figure 5-14: Link budget Analysis Simulation Result

As for the harmonic balance simulation of the receiver, the schematic is shown in Figure 5-15. Harmonic balance simulations result shows that the amplitude of received signal is higher at intended frequency 70MHz and other nonlinear harmonics have lower amplitudes which is as expected. This result is shown in Figure 5-16.

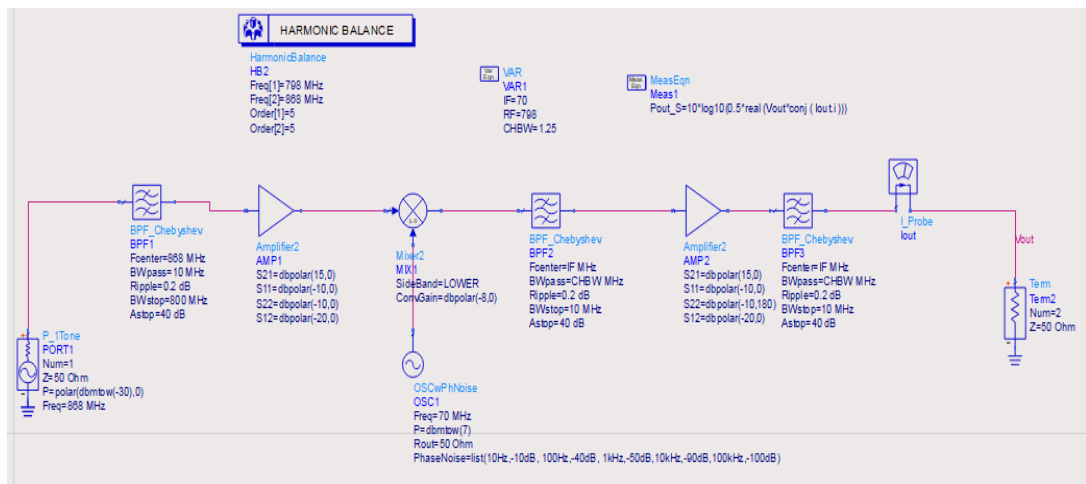


Figure 5-15: Harmonic Balance Simulations Schematic Diagram

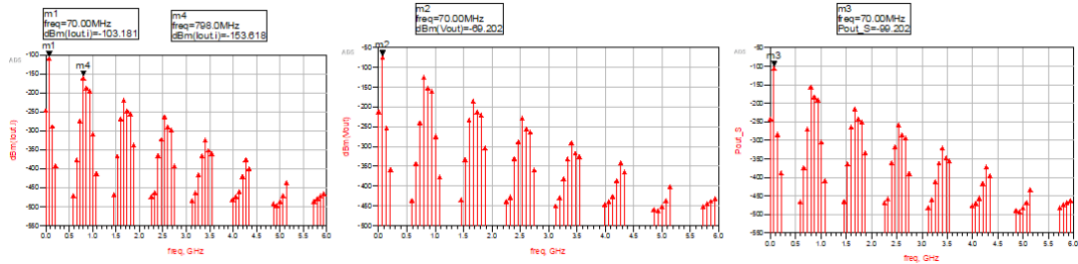


Figure 5-16: Harmonic Balance Simulation Result

For s-parameters simulations of receiver circuit the schematic is shown in Figure 5-17. The input power to the receiver is -30dBm, gain of LNA is kept at 45dB. As for the pass band of BPF it is 10MHz with central frequency of 868MHz. The signal then passes to the mixer down converting the 868MHz signal to IF signal. After down conversion there is another filter to pass only the intended IF signal and filter out the other harmonics produced by the mixer. After that there is an amplifier of gain 45dB. At the last BPF, only the intended IF signal will be passed. This is shown in the results in Figure 5-18.

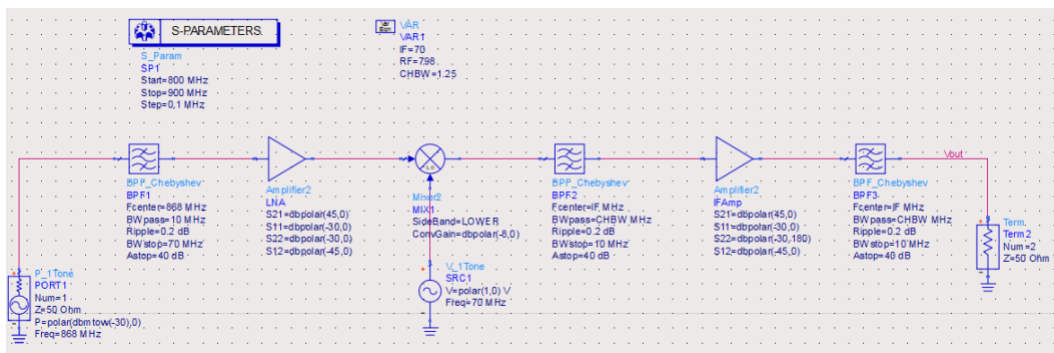


Figure 5-17: S-parameter Simulation Schematic Diagram

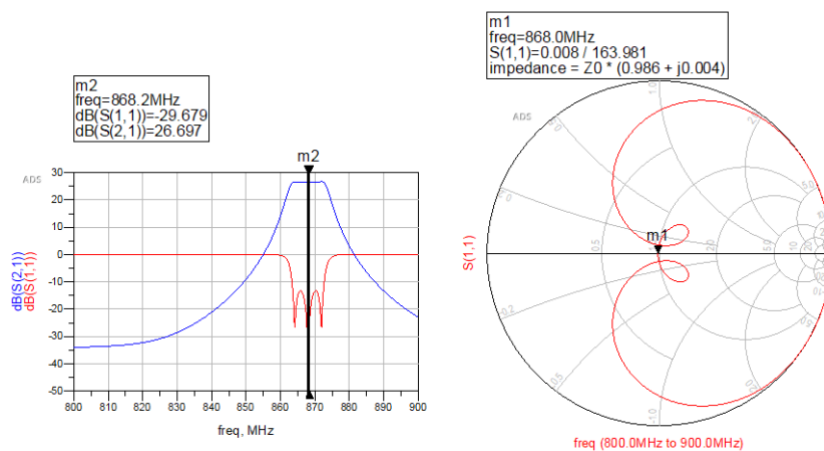


Figure 5-18: S-parameters Simulation Result

5.3. Transmitter Analysis and Results

The s-parameters simulation for the transmitter chain has been designed as is shown in Figure 5-19. IF signal of 70MHz is up converted through mixer of 868MHz frequency. The signal is based through a BPF in order to pass the desired signal and filter out the other unwanted harmonics introduced. The next stage is a two-stage amplification to amplify the up converted signal. This signal will then pass through the BPF.

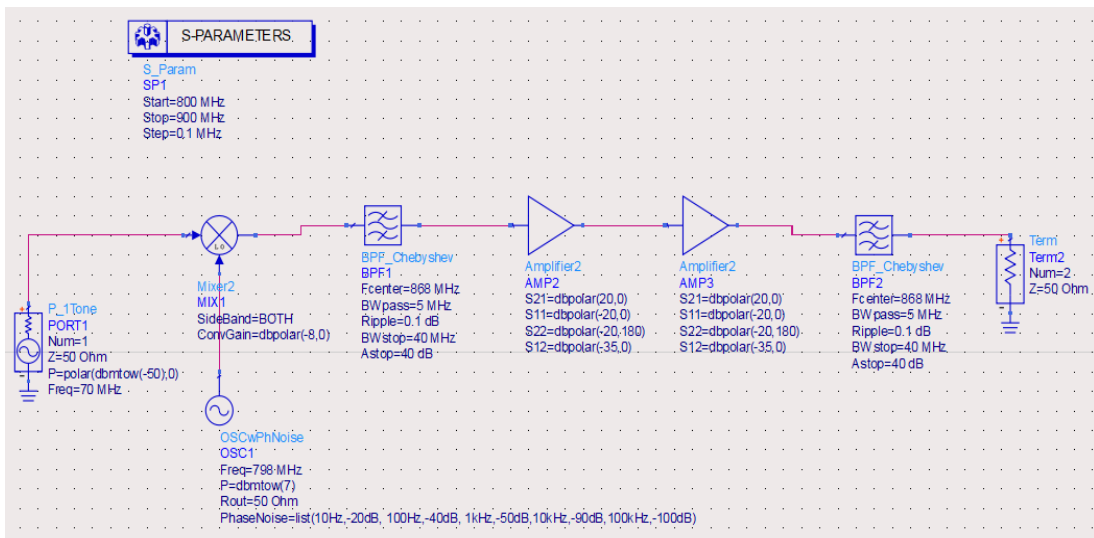


Figure 5-19: S-parameter Simulation of Transmitter Schematic Diagram

The simulation result in Figure 5-20 shows that the output signal from transmitter has a center frequency of 70MHz with amplitude around 58dB.

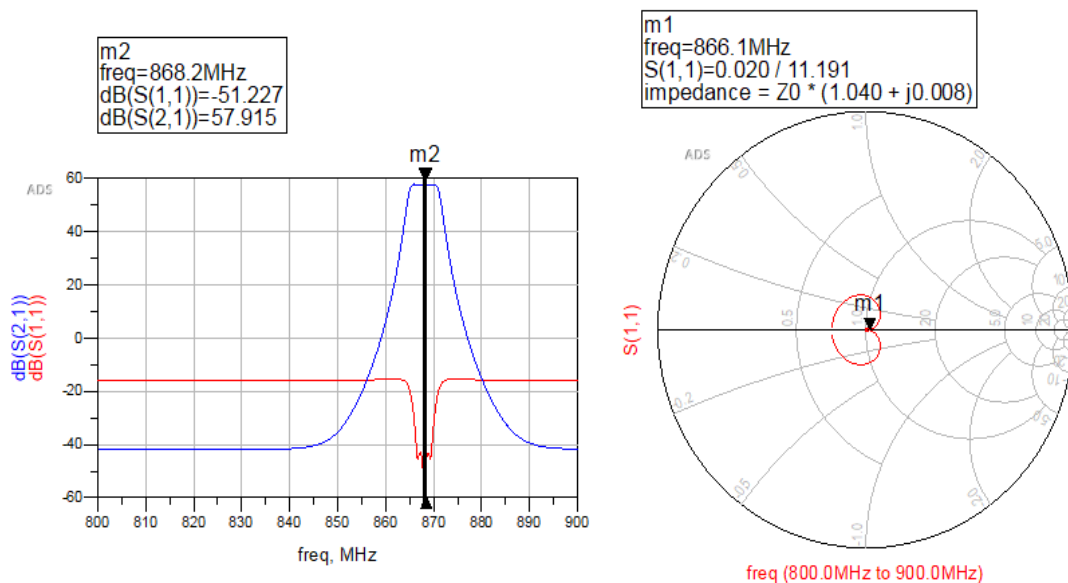


Figure 5-20: Simulation Result for S-Parameters

As for the link budget analysis the design has been implanted in the schematic shown in Figure 5-21. Along with that, a budget analysis block has been placed in the schematic.

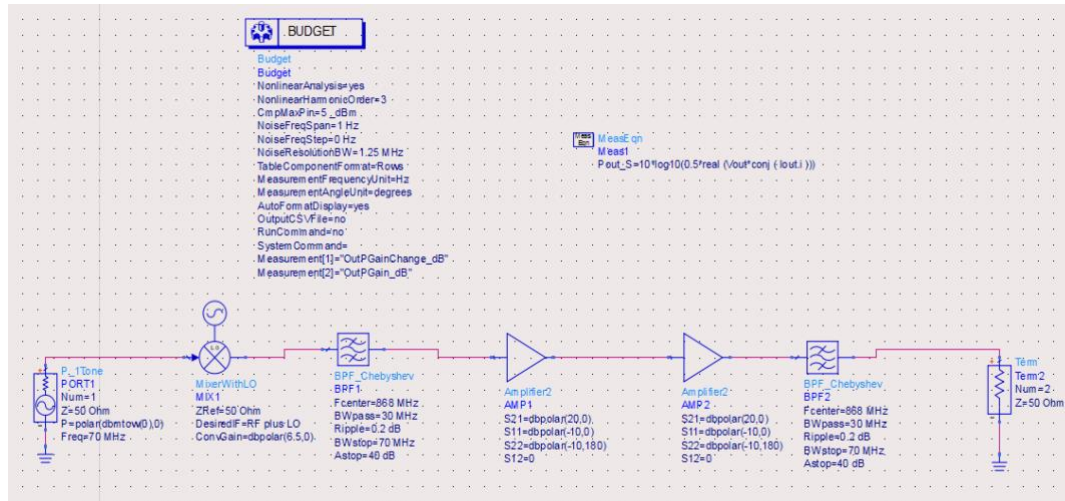


Figure 5-21: Link Budget Analysis Schematic Diagram

The simulation result reveals that the signal up converted from the mixer has amplitude level of 5.8dB. the BPF introduced insertion loss and the signal level goes down to 4.6dB. After that there are two power amplifiers, which amplifies the signal up to 43.9dB. Finally, the BPF introduces an insertion loss of 1dB which makes the final amplitude of the output signal is 42.9dB.

The harmonic balance simulations of the transmitter are shown in the Figure 5-22 and Figure 5-23.

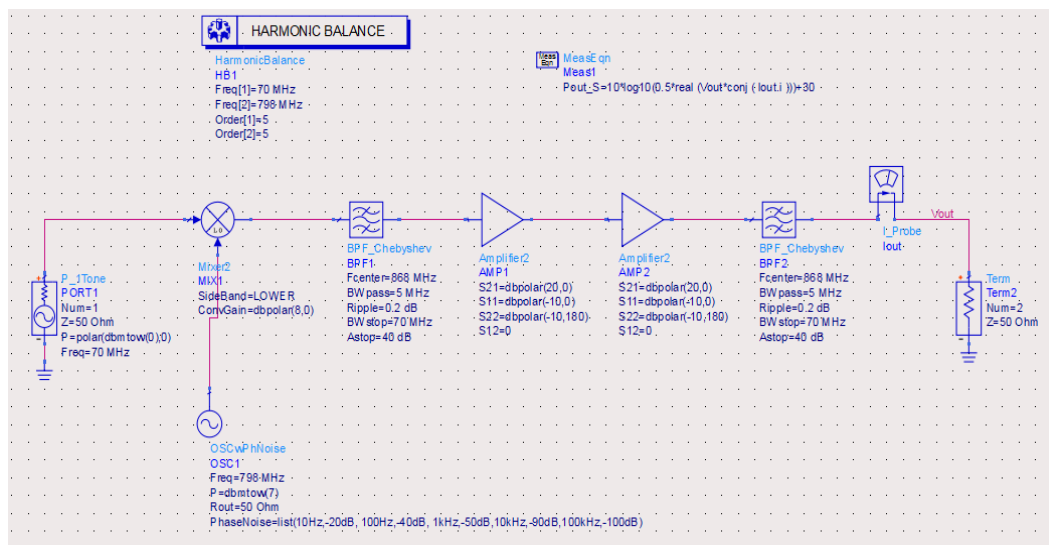


Figure 5-22: Harmonic Balance Simulations Schematic Diagram

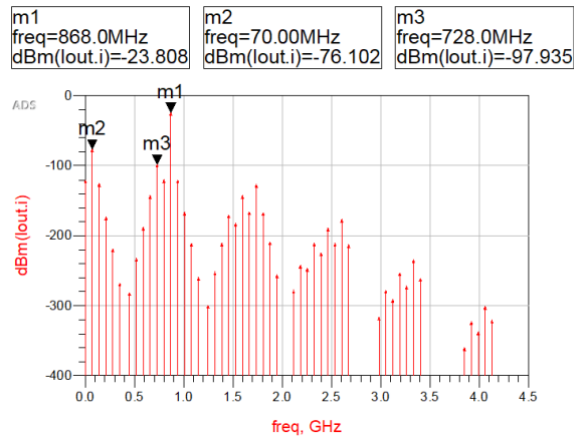


Figure 5-23: Simulation Result

As of the output voltage, the current and the power of the intended signal from the harmonic balance simulations, all are shown in Figure 5-24

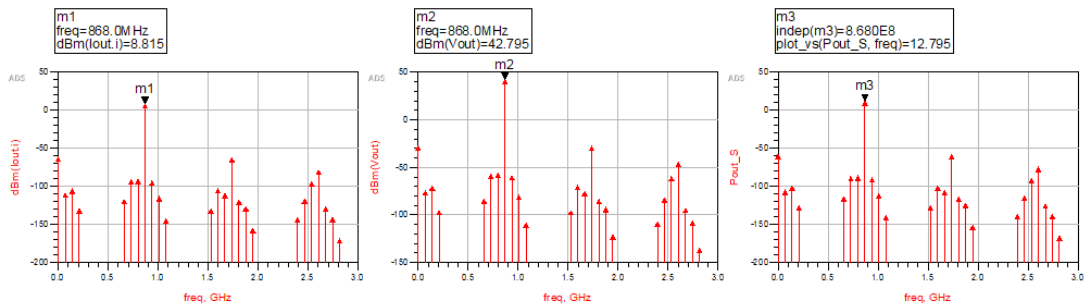


Figure 5-24: Simulation Results

5.4. Antenna Analysis and Results

HFSS tool has been used to design and simulate the antenna. The designed antenna is shown in Figure 5-25 with a simulation result to illustrates the return loss. This shows that the antenna does operates at 868MHz with good matching to 50Ohm port as shown in Figure 5-26.

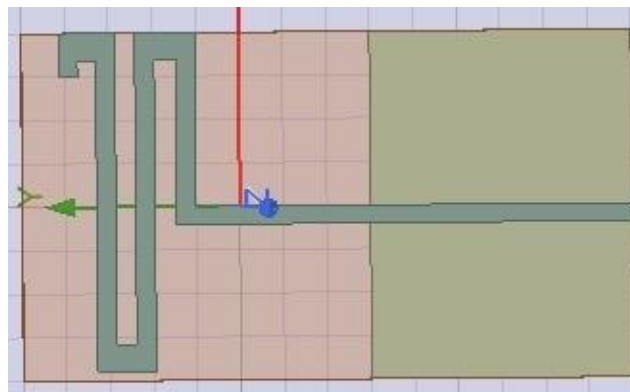


Figure 5-25: Antenna Design in HFSS

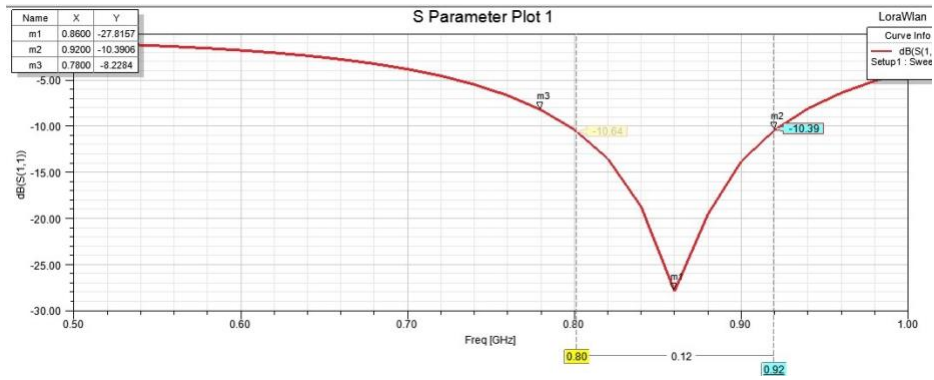


Figure 5-26: S-Parameters Simulation Result

The VSWR has also been analyzed in order to validate the functionality of the antenna at the frequency of 868MHz. As shown in Figure 5-27, the graph of the Voltage Standing Wave Ratio is 1.0848 at the entitled frequency which is less than 2. This makes the antenna effectively matched to transmission line. Adding to that, a 3D radiation pattern shows that the antenna designed is an omnidirectional antenna which radiates the signal in two dimensional plane equally as shown in Figure 5-28.

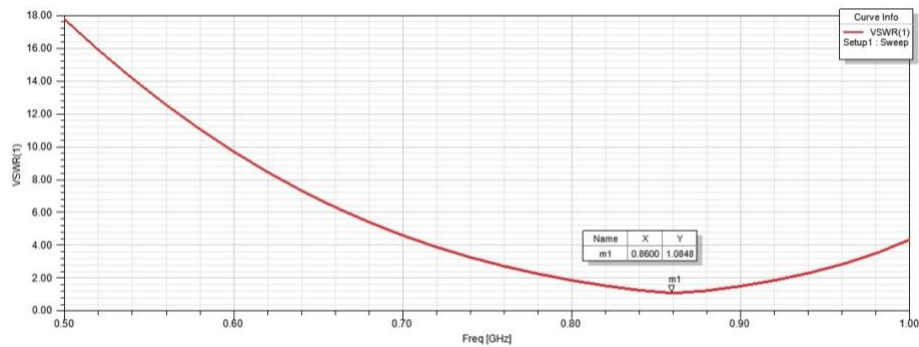


Figure 5-27: VSWR

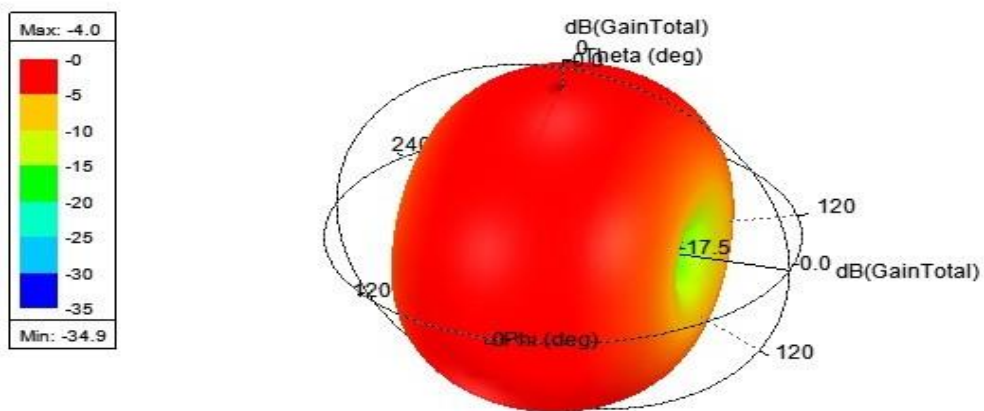


Figure 5-28: 3D Radiation Pattern of The Designed Antenna

Chapter 6. Conclusion and Future Work

In this thesis, a major issue of CubeSat that the market is facing has been highlighted. The issue of the very high cost of launching any space solutions makes it hard for everyone to contribute and have access to the space. This high cost can be reduced if the mass of the CubeSat has been reduced as it is directly proportional to each gram of the CubeSat. The mass of this CubeSat comes from three main elements: subsystems, structure, and harness. So many developers are trying to reduce the mass of the harness by changing the isolation and the materials used, however, there is still approximately a 20% mass contribution to the overall mass from the harness.

For this reason, a new design of transceiver board to replace the harness of a spacecraft has been presented. This transceiver board is responsible for sending and receiving all the data whether it is telemetry or commands between all the subsystems within the CubeSat. Those data are collected through I2C by the microcontroller then gets processed and sent to the transceiver through the SPI. The transceiver will packetize it into LoRa Protocol format ready to be sent to the other subsystem through the ISM ceramic antenna. The mass contribution of this solution is 2 grams per board. For a 1U CubeSat with 5 subsystems, then the contributed mass will be 10 grams. On the other hand, the added power consumption per board will be 83mW on transmission mode and 0.05mW on the sleep mode.

The design of this transceiver PCB has been implemented using Altium Design tool by using actual components that exists in the market. Those components have been chosen carefully to satisfy all the design requirements. In this design we are optimizing the power and the mass to adapt to any future spacecraft design. In Order to verify the design an analysis has been conducted using ADS tool in order to show the Radio Frequency design performance.

This transceiver design is designed in a way that can adapt to different protocol and scheme as needed. This can allow different usage of this transceiver not only as a harness replacement. An example of other usage is using it as a testing tool while the spacecraft is still on ground during functional and operation test. The current design is used to send and receive data within the CubeSat and can be used within any spacecraft. However, if the RF power signal will be increased, this transceiver can be utilized in

satellite constellation projects. It will be the link between those constellation satellite while in space instead of using the ground station intervention with all of them.

References

- [1] European for Space Standardization, "Space product Assurance - Derating - EEE Components," ECSS-Q-ST-30-11C REV 1, *ECSS Secretariat ESA-ESTEC - Requirements & Standards Division -Noordwijk, The Netherlands*, Chapter 6.32, October 2011.
- [2] "Space Transportation Costs: Trends in Price Per Pound to Orbit ..." *yumpu.com. Futron Corporation*. Retrieved 3 January 2021.
- [3] Rogers and C. Plett, *Radio frequency integrated circuit design*. Boston: Artech House, 2010, pp. 123-35.
- [4] "What Is It? - Lora Alliance®," Internet: www.lora-alliance.org/wp-content/uploads/2020/11/what-is-lorawan.pdf, Nov. 2015. [Mar. 23,2020].
- [5] S. -Y. Wang *et al.*, "Performance of LoRa-Based IoT Applications on Campus," *2017 IEEE 86th Vehicular Technology Conference (VTC-Fall)*, 2017, pp. 1-6.
- [6] "CubeSat101 Basic Concepts and Processes for First-Time CubeSat Developers",Internet: https://www.nasa.gov/sites/default/files/atoms/files/nasa_csli_cubesat_101_508.pdf, 2019 [Dec. 18, 2019].
- [7] "PC /104 specifications", Internet: https://pc104.org/wp-content/uploads/2015/02/PC104_Spec_v2_6.pdf, 2019 [Dec. 18, 2019].
- [8] A. Williams, J. Puig-Suari and M. Villa, "Low-cost, low mass avionics system for a dedicated Nano-Satellite launch vehicle," *2015 IEEE Aerospace Conference*, 2015, pp. 1-8.
- [9] Y. Su, Y. Liu, Y. Zhou, J. Yuan, H. Cao and J. Shi, "Broadband LEO satellite communications: Architectures and key technologies", *IEEE Wireless Communications*, vol. 26, no. 2, pp. 55-61, Apr. 2019.
- [10] A. Junge, J. Wolf, N. Mora, F. Rachidi and P. Pelissou, "Electromagnetic interference control techniques for spacecraft harness," *2014 International Symposium on Electromagnetic Compatibility*, 2014, pp. 1-8.
- [11] M. R. Hayhurst, D. C. Judnick, R. E. Bitten, I. E. Hallgrimson, S. A. Shinn and M. A. Youngs, "Historical mass, power, schedule, and cost growth for NASA spacecraft," *2016 IEEE Aerospace Conference*, 2016, pp. 1-17.
- [12] X. Wang and S. Zhang, "Cost Analysis for Mass Customized Production of Satellites Based on Modularity," in *IEEE Access*, vol. 9, pp. 13754-13760, 2021.

- [13] A. G. Accettura and M. Genito, "Vega launch vehicle options to serve different satellites markets," *2012 IEEE First AESS European Conference on Satellite Telecommunications (ESTEL)*, 2012, pp. 1-4.
- [14] S. Wiens and K. Epstein, "Low cost deployment of auxiliary payloads," *2000 IEEE Aerospace Conference. Proceedings (Cat. No.00TH8484)*, 2000, pp. 329-334 vol.4.
- [15] I. R. McNab, "Preliminary study on the EM launch of nano-satellites," *2017 IEEE 21st International Conference on Pulsed Power (PPC)*, 2017, pp. 1-4.
- [16] J. Puig-Suari, C. Turner and W. Ahlgren, "Development of the Standard CubeSat Deployer and a CubeSat Class PicoSatellite", *2001 IEEE Aerospace Conference Proceedings (Cat. No.01TH8542)*, 2001, pp. 1/347-1/353 vol.1.
- [17] W. Huang, J. Loman, R. Andrada, M. L. Hanson and D. Borja, "An Optimal Two-Stage Launch Plan of a Satellite Constellation to Maintain Mission Reliability Requirement," *2018 Annual Reliability and Maintainability Symposium (RAMS)*, 2018, pp. 1-7.
- [18] V. R. Srivastava et al., "Modular Power System and bus bar scheme in high power communication satellite," *2014 IEEE Electrical Design of Advanced Packaging & Systems Symposium (EDAPS)*, 2014, pp. 45-48.
- [19] W. A. Watson, "Rapid spacecraft development: results and lessons learned," *Proceedings, IEEE Aerospace Conference*, 2002, pp. 7-7.
- [20] H. Heidt, J. Puig-Suari, A. Moore, S. Nakasuka and R. Twiggs, "CubeSat: A new Generation of Picosatellite for Education and Industry Low-Cost Space Experimentation", *14th AIAA/USU Conference on Small Satellites*, 2000, pp. 1-19.
- [21] SEMTECH, "Application Note: Recommendations for Best Performance" AN1200.37, Jan 2018
- [22] "CubeSat AIS receiver," Internet: <https://nanoavionics.com/cubesat-components/cubesat-ais-receiver/>, Jan. 11, 2022 [Mar. 16, 2022].
- [23] "CubeSat S-band transceiver," Internet: <https://nanoavionics.com/cubesat-components/cubesat-s-band-transceiver/>, Jan. 11, 2022 [Mar. 16, 2022].
- [24] "S-band Transceiver I - Cubesat Communication," Internet: <https://www.endurosat.com/cubesat-store/cubesat-communication-modules/s-band-transceiver/>, Mar. 11, 2022 [Mar. 16, 2022].
- [25] "UHF Transceiver II Cubesat communication," Internet: <https://www.endurosat.com/cubesat-store/cubesat-communication-modules/uhf-transceiver-ii/#request-step-modal>, Mar. 4, 2022 [Mar. 16, 2022].

- [26] “Isis TXS high data rate S-band transmitter,” Internet: <https://www.cubesatshop.com/product/isis-txs-s-band-transmitter/>, Dec. 29, 2021 [Mar. 16, 2022].
- [27] “Isis UHF downlink/VHF uplink full duplex transceiver,” Internet: <https://www.cubesatshop.com/product/isis-uhf-downlink-vhf-uplink-full-duplex-transceiver/>, Dec. 29, 2021 [Mar. 16, 2022].
- [28] “Totem nanosatellite SDR platform,” Internet: <https://www.cubesatshop.com/product/totem-nanosatellite-sdr-platform/>, Nov. 19, 2021 [Mar. 16, 2022].
- [29] “Bluetooth Protocol – Type, Data Exchange and Security,” Internet: <https://www.elprocus.com/bluetooth-protocol-types-and-data-exchange/>, 2013 [Mar. 21, 2022].
- [30] B. Chaudhari and S. Borkar, “Design Considerations and Network Architectures for Low-Power Wide-Area Networks,” in *LPWAN Technologies for IoT and M2M Applications*, pp. 15-35, 2020.
- [31] “FAQ,” Internet: https://developer.sony.com/develop/spresense/docs/faq_en.html#:~:text=What%20is%20Spresense%3F,power%20consumption%20application%20processor%20cores, 2022 [Mar. 21, 2022].
- [32] “GSMA: Low Power Wide Area Technologies,” Internet: <https://www.gsma.com/iot/wp-content/uploads/2016/10/3GPP-Low-Power-Wide-Area-Technologies-GSMA-White-Paper.pdf>, 2021 [Mar. 21, 2022].
- [33] “Internet of Things,” Internet: <https://www.gsma.com/iot/narrow-band-internet-of-things-nb-iot/>, 2021 [Mar. 21, 2022].
- [34] L. Rob. “Comparing IoT Connectivity with LoRa, Cellular, and Wi-Fi,” Available: <https://blues.io/blog/network-connectivity/>, Apr. 12, 2021 [Mar. 21, 2022].
- [35] “LTE Encyclopedia,” Internet: <https://sites.google.com/site/lteencyclopedia/home>, 2021 [Mar. 21, 2022].
- [36] “LTE Quick Reference,” Internet: https://www.sharetechnote.com/html/Handbook_LTE_NB_LTE.html, 2020 [Mar. 21, 2022].
- [37] S. Ralph and G. Reynolds. *Principles of Information Systems*. New York, NY: Cengage Learning, 2020.
- [38] “Spresense Main Board: CXD5602 Microcomputer for IoT Application,” Internet: <https://www.seeedstudio.com/Spresense-Main-Board-CXD5602-Microcomputer-for-IoT-Application-p-2846.html>, 2022 [Mar. 21, 2022].

[39] “*The Bluetooth Protocol Architecture,*” Internet: <https://www.tutorialspoint.com/the-bluetooth-protocol-architecture>, Mar. 23, 2020 [Mar. 23, 2022].

[40] “*What are LoRa and LoRaWAN?*” Internet: [https://lora-developers.semtech.com/documentation/tech-papers-and-guides/lora-and-lorawan/#:~:text=The%20name%2C%20LoRa%2C%20is%20a,areas%20\(line%20of%20sight\)](https://lora-developers.semtech.com/documentation/tech-papers-and-guides/lora-and-lorawan/#:~:text=The%20name%2C%20LoRa%2C%20is%20a,areas%20(line%20of%20sight)), 2020 [Mar. 21, 2022].

[41] “*What Is Zigbee?*” Internet: <https://www.digi.com/solutions/by-technology/zigbee-wireless-standard#:~:text=Zigbee%20is%20a%20wireless%20technology,900%20MHz%20and%20868%20MHz>, 2019 [Mar. 21, 2022].

[42] “*ZigBee Technology Architecture and Its Applications,*” Internet: <https://www.elprocus.com/what-is-zigbee-technology-architecture-and-its-applications/>, 2019 [Mar. 21, 2022].

Vita

Hessa Ali was born in 1993, in Dubai, United Arab Emirates. She received her primary and secondary education in Dubai, UAE. She received her B.Sc. degree in Electrical Engineering from the American University of Sharjah in 2015 with a minor in Renewable Engineering. From 2015 until 2018 she worked as a satellite avionics Engineer for Emirates Mars mission and from 2018 until now, she works as project management engineer in Mohammed Bin Rashed Space Center (MBRSC).

In 2017 she joined the Electrical Engineering master's program in the American University of Sharjah. Her research interests are in satellite, space, and modern transceivers.